Università Politecnica delle Marche
Scuola di Dottorato di Ricerca in Scienze dell'Ingegneria
Corso di Dottorato in Ingegneria Industriale

Non-contact smart measurement systems for in-line quality control of precision turned parts

Ph.D. Dissertation of:
Matteo Fitti

Supervisor:
Prof. Nicola Paone

Assistant Supervisor:
Dr. Paolo Chiariotti

Ph.D. Course coordinator:
Prof. Giovanni Di Nicola

XVIII edition - new series

Abstract

This thesis is the result of work carried out within the European project H2020 GO0D MAN and intends to be a contribution to realize the Industry 4.0 paradigm. In particular, it concerns the development of in-line smart quality control systems.
The work presents the development of two systems: a) an automated measurement system based on a confocal chromatic sensor for checking the dimensions of turned metal components and b) an automated control system based on computer vision for checking the presence of burrs due to the drilling process on the same parts.
These metal components, which consist of little hollow cylinders with several lateral holes, are used in hydraulic valves intended for use in the automotive industry. The quality control of these parts requires the verification of stringent dimensional tolerances and functional performances. The overall objective of the project is to realize an in-line 100% quality control in order to prevent the generation and propagation of defects at the exit of the turning processing station.
The two systems developed exhibit smart behaviour, aimed at managing measurement uncertainty and reducing the risk of misdiagnosis. The automation level and the optical non-contact approach adopted allows to extend the controls previously made on statistical samples to 100% of the production.
After presenting the industrial cases, this thesis discusses the conceptual design for each system, the steps for the realization of the prototypes, their characterization in laboratory condition and finally the demonstration in a real production line.

Contents

List of Figures

List of Tables

Chapter 1

Introduction

Manufacturing industries are currently facing new challenges given by the Industry 4.0 paradigm. Indeed, the disruptive impact provided by digitalization is requiring a constant evolution towards new technologies able to rapidly adapt both processes and products.

In-line quality control is recognized as one of the pillars of digital factories, according to the paradigm of Industry 4.0; indeed, early detection of defects and anomalies allows preventing defects to propagate to downstream processes and allows to develop adaptive control strategies which may compensate for deviations from nominal specifications by feed-back at single process or feed-forward at following stages of a multistage manufacturing system. Therefore, quality control is intimately connected to process control [25], in the perspective of Zero Defect Manufacturing (ZDM) [55].

In this context, it becomes clear that a zero-defect strategy requires reliable information to support any decisions. Reliable information requires measured data from the process and the product. In a real production scenario, however, the availability of data does not by itself guarantee an effective information build-up. In particular, measurement uncertainty must be known, kept under control and adequately managed so to keep the confidence level on measured data at the required level and therefore to effectively support the following decision making based on data.

These measurement systems are aimed at supporting in-line quality control, which consists of taking measurements in-line, possibly on 100% of the production, process data to extract characteristic features and perform a diagnosis by assessing compliance to specifications or identifying and classifying defects. Quality control is a decision-making process, for which uncertainty of measurement plays a fundamental role; if data are uncertain, the following diagnosis may be uncertain too. Smart Quality Control Systems (QCS) are designed to exhibit real-time adaptive behaviours, in order to keep measurement uncertainty under control even in case of variations of process/product parameters; they could implement data pre-processing to derive synthetic quality indicators, self-diagnosis and self-calibration to maximize the confidence level of the sensors output.

The European Commission is devoting large efforts to promote research [4] and innovation in the sector of manufacturing, with a particular focus on smart factories, the so-called factories of the future, and the associated technologies. In particular, in Horizon 2020, several Calls have been opened in the last years, also through the actions of the Public Private Partnership EFFRA (European Factories of the Future Research Association, [2]) and of the Technology Platform Manufuture ([5]). These associations, after consultation with their industrial partners, provide the EU Commission with road-maps and a vision towards the development of advanced manufacturing. They represent the stakeholder in the manufacturing sector.

This research is part of the European Project GO0D MAN-"aGent Oriented Zero Defect Multi-Stage Manufacturing" [3]. GO0D MAN project has received funding from the European Commission under the EU Framework Programme for Research and Innovation Horizon 2020 (2014 - 2020) within the FoF – Technologies for Factories of the Future initiative. Contract no. H2020-FOF-03-2016-723764.

A cluster of European projects, of which GO0D MAN is part, has formed the Zero Defect Manufacturing (ZDM), a sub-platform of Manufuture. The topic of in-line quality control is of course strictly connected to ZDM.

The thesis is organised as follows. Chapter 2 provides an overview of GO0D MAN European Project: the distributed system architecture and the three use cases' characteristics. The last part of this chapter describes the Zannini production scenario and the two quality control systems to develop.
Chapter 3 discusses the Confocal chromatic sensor quality control system for geometric feature assessment. Its first part is dedicated to the state of the art of this particular measurement inspection and of the confocal chromatic sensor. In the second part, the hardware design and realization are discussed in detail. In the third part, the smart behaviours and software are presented. In the last two parts, the metrological laboratory performances and the results in a real production scenario are reported.
Chapter 4 describes the quality control system for burrs identification. The first part introduces the state of the art of this inspection. The two following parts are focussed on the hardware and software development of the quality control system. The last part of this chapter analyses the results of the system in the production environment.
Chapter 5 draws the conclusions of the entire work.

Chapter 2

Inline quality control in the field of Industry 4.0

2.1 GO0D MAN Architecture

The core idea of the GO0D MAN project is to integrate and combine process and quality control for a multi–stage manufacturing production [25, 16] into a distributed system architecture built on agent-based Cyber-Physical Systems (CPS) [1] and smart inspection tools. This framework, based on agents associated to each process and to each product, supports real-time data collection and defect diagnosis at single process level, as well as inter-stage sharing and processing of information at global level using data mining techniques. The Zero Defect Manufacturing (ZDM) strategy proposed by the GO0D MAN project runs on this framework, at local and at global system level, has been demonstrated in three relevant industrial cases with multi-stage production lines with different levels of automation and production rate.
The real time and early identification of deviations and trends, performed at local level, allow to prevent the generation of defects at single stage and their propagation to down-stream processes, enabling the global system to be predictive (early detection of process faults) and proactive (self-adaptation to different conditions).
Multistage manufacturing systems are inherently complex because of their hybrid structures with mixed sequential and/or parallel stages, mixed data types and scales and the existence of feedback/forward loops. In multistage systems the outputs from a given stage are the inputs to another, result from one stage is influenced by local variations in the process, but also by the propagation of defects from the previous stages, hence the overall global performance of these systems is statistically dependent on the stochastic performance of each individual stage. Traditional approaches for quality control, which are mainly based on Statistical Process Control (SPC) treat the multi-stage system as a whole and lack the capability to discriminate among changes at different stages. First, the statistical models and process distributions are assumed known and cannot be defined properly in the multidimensional space. Second, the large amount of data generated/used in a multistage system cannot be processed efficiently using traditional processing methods. This implies the need for combining model and data-driven approaches in quality control.

The Zero Defect Manufacturing framework for multi-stage production employs the following technologies:

1. Integration of process control and quality control by using an agent-based CPS architecture. The choice of this solution is motivated by its intrinsic characteristics e.g., distribution, decentralization, modularity and robustness, which are particularly suited to implement control at local and global levels in multi-stage manufacturing, to achieve modularity, to develop adaptation and reconfigurability whilst reducing complexity.

2. Quality control systems (QCSs) designed to exhibit at local level (single stage: process operation, quality control station) real-time adaptive behaviors to keep measurement uncertainty under control [58, 45] even in case of variations of process/product parameters, pre-process

data to derive synthetic quality indicators, implement self-diagnosis and self-calibration to maximize the confidence level of the sensors output.

3. Data-driven approaches supported by advanced ICT and big data analytics tools for real-time data processing and analysis by data mining at both local and global levels. These features enable real-time and early detection of process/product quality deviations and trends, establish correlations between upstream and downstream process variables so to allow updating downstream process parameters and acceptance thresholds for quality checks.

The GO0D MAN EU project is structured on a distributed system architecture where hardware and software components perform specific functions at different levels and information and data are exchanged between levels (Figure 2.1).

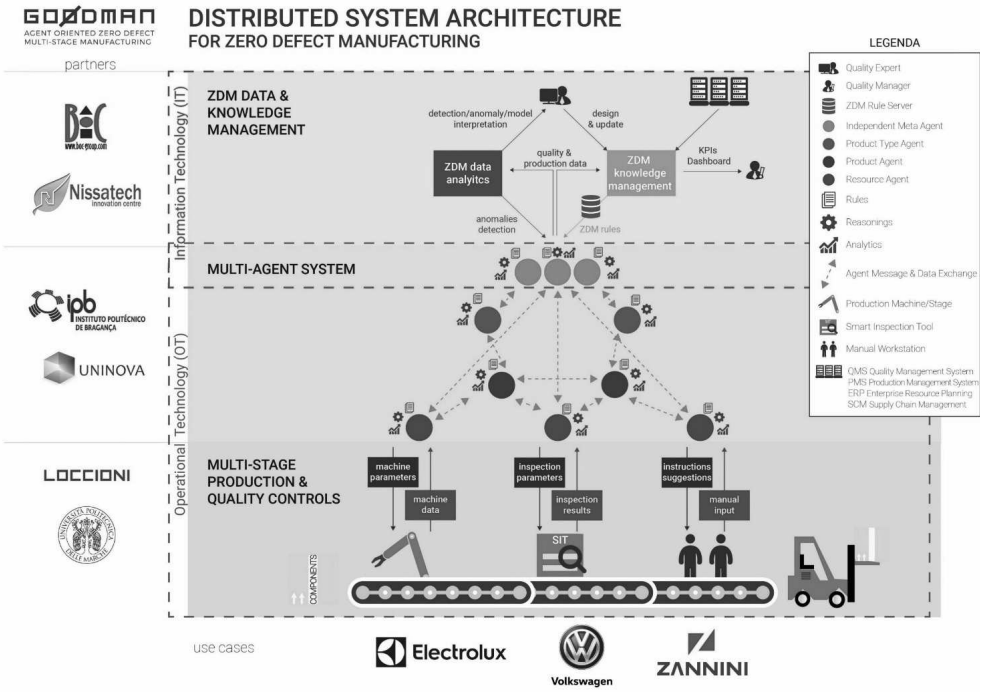

Figure 2.1: Manufacturing system architecture according to GO0D MAN vision

The three main levels of this system are: a bottom level, which is the operational technology (OT) level, involving the production line and the quality control systems, i.e. the physical resources operating on the shop floor; a central level, ruled by the Multi-Agent-System (MAS) structure [39], that allows CPSs to interact; a top level, the Information Technology (IT) level, representing the decision layer grounding on data analytics and knowledge management.

The three use cases of the GO0D MAN project are representative of a large share of production scenarios that are common in manufacturing. They differ in modes of operation, in production rate and have a significant and different level of automation and involvement of human operators.

The use case of Volkswagen Autoeuropa represents a typical automotive production system, in particular the car body assembly. We are considering the tail-gate and the rear head-lights assembly. This section of the whole assembly line is characterized by a serial assembly of the parts while the car body is slowly moving on a transport belt; assembly is performed by operators, manually or with the support of simple tools. In several stages the operators mount the tail gate and the head-lights, according to a pre-set sequence to be performed within a time window set by the fixed takt time of the line. The alignment of parts being assembled is the most relevant requirement; this implies the measurement of the gap&flush, which today is done manually by a hand-held feeler gauge. No data is acquired nor stored. Each car body being produced is uniquely identified and tracked along the line. There is the need to acquire gap&flush data during the assembly process, with the purposes of providing feed-back and guidance to the operators and of

storing data associated to each car body produced. This need has led to the requirement to develop a portable hand-held gap&flush measurement device.

The use case of Zannini represents a typical batch production system, in particular the serial production of small high-precision turned metal parts, produced in rather large batches by automatic tooling machines. The parts are subject to strict geometrical specifications, in the micrometric range. Furthermore, it is strictly required that no burrs are left inside the parts after the production. In this type of multistage production system quality control is performed by statistical approach; samples are taken from each batch and brought to the metrology laboratory for off-line inspection and measurement. Data are then processed according to state-of-art Statistical Process Control (SPC) and results associated to the batch from which the samples were extracted. There is the need to take geometric measurements in-line, increasing the sampling rate possibly to 100% and to inspect all parts for the presence of burs. These needs have led to the requirement to develop the set of measuring systems to be inserted at different stages of the production line.

The use case of Electrolux Professional represents the production of personalized products, in particular professional ovens. This product is realized in hundreds of variants on the same line, where most of the assembly operations are manual. Production rate is very low and each oven is identified individually. At present, 100% quality control is performed only at the end of the line on the finished product, by specific test cycles aimed to verify compliance to technical specifications and functional performance. No measurements are taken at the previous assembly stages. There is the need to perform quality controls before the final assembly, at upstream assembly stages. This need has led to the selection of new quality controls to be developed for this case.

The Measurement group at Università Politecnica delle Marche (UNIVPM) wherein I carried out my PhD activity has been responsible on the development of quality control systems at the bottom level of the GO0D MAN distributed system architecture. QCSs represent local CPS which are fundamental to make possible a zero-defect strategy, because they are the nodes of the system where data are measured and quantitative information takes origin, and where diagnosis on each process performance is done. The following data analytics and knowledge management relies on the quality of the information, hence on the metrological performance of the QCSs.
Figure 2.2 shows all the QCSs developed within GO0D MAN EU project.

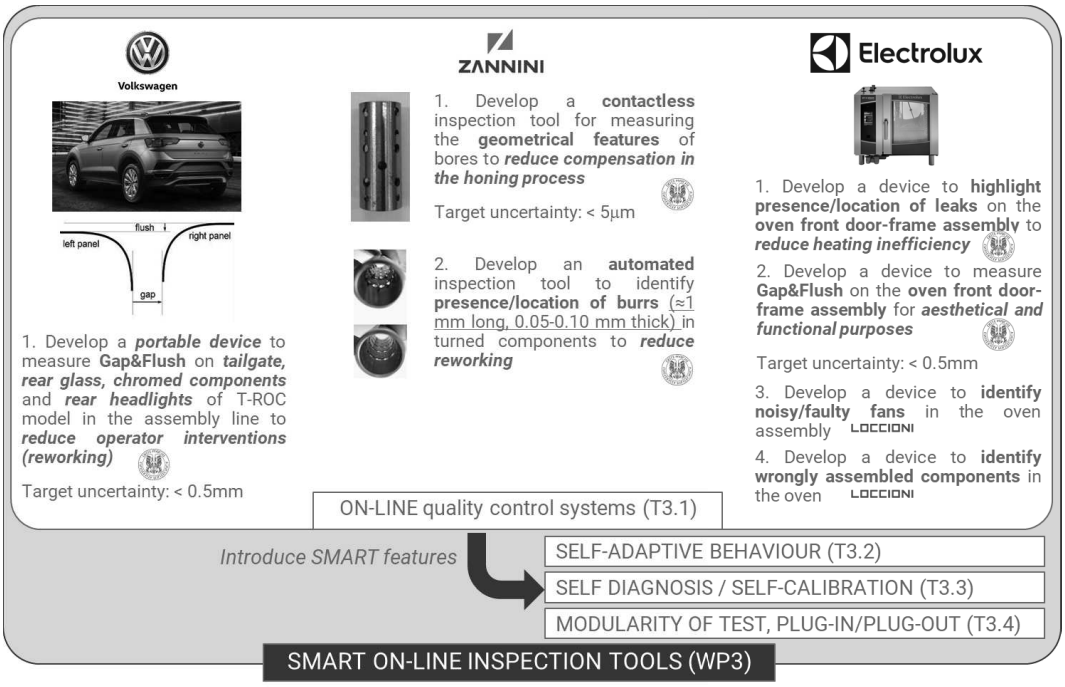

Figure 2.2: List of prototype smart inspection tools developed within GO0D MAN EU project

Within GO0D MAN my role has been to develop two new QCSs for the Zannini use case.

2.2 Zannini Use Case

The ZANNINI Group is made of four companies active in the field of precision machining, with focus on turned metal components. The ZANNINI group participated GO0D MAN as Zannini Poland and Zannini Spa, respectively responsible for the demonstration phase and the R&D activity of the Group within the project. Zannini specialises in high technology products covering several industry sectors such as automotive and household appliances, and produces high precision mechanical components for hydraulic and pneumatic systems.
Figure 2.3 shows Zannini plants located in Europe and their key charachteristics.

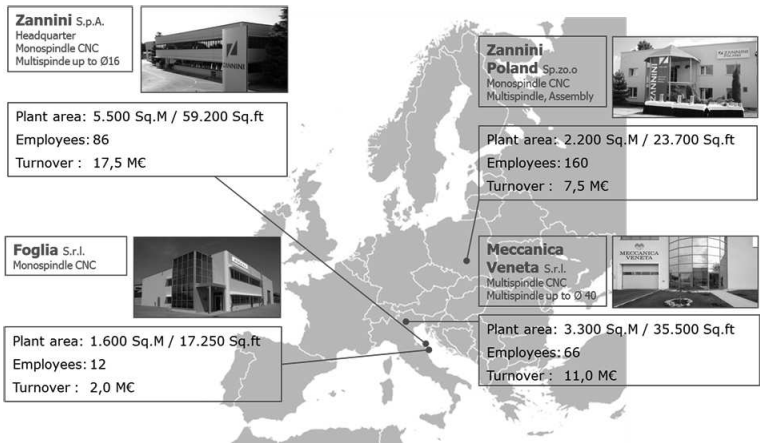

Figure 2.3: Zannini in Europe

The plant where GO0D MAN demonstration has been developed is in Poland. In Zannini Poland plant (Figure 2.4) there are about 36 production machines including: turning machines (sliding and fixed headstock, mechanical and Computer Numerical Control (CNC), mono-spindle and multi-spindle), grinding machines, honing machines, hard turning machines, secondary operation machines (induction hardening, sand blasting, transfer, thermal deburring, washing, etc.), assembly lines.

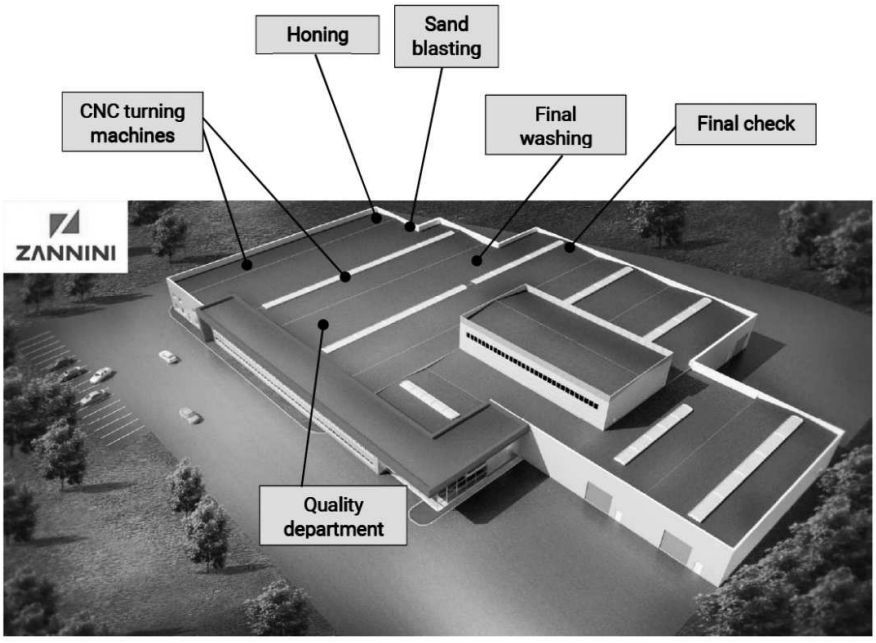

Figure 2.4: Zannini Poland plant

Some of the CNC machines are illustrated in Figure 2.5.

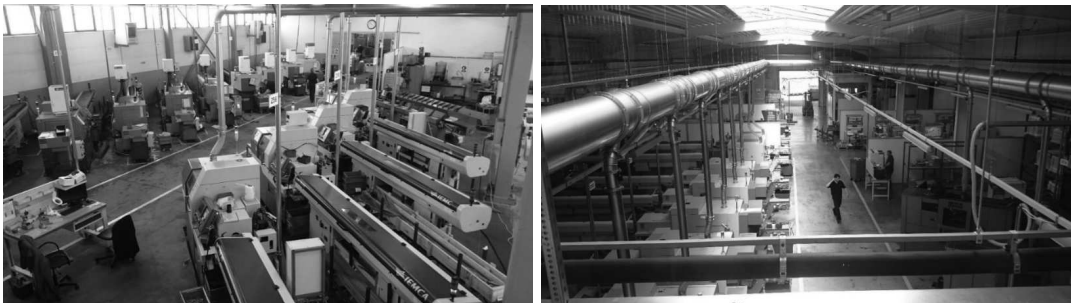

(a) (b)

Figure 2.5: Zannini's Equipment

The multi-stage production process (Figure 2.6) includes the following machining operations: turning, deburring, honing and washing.

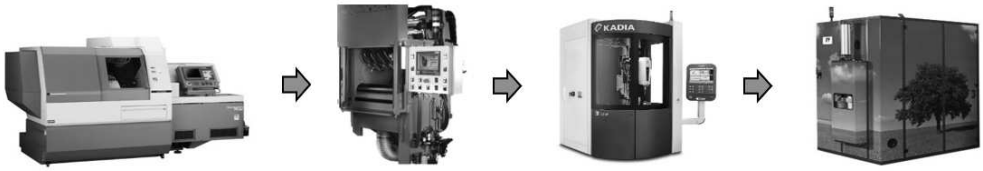

Figure 2.6: Zannini Production Process

The main machining processes are turning and honing; between them deburring occurs, by sand blasting, necessary to delete burrs from the pieces.
The turning operation is the removal of metal from a rotating cylindrical workpiece. It allows to obtain a cylindrical net-final shape, having a relatively accurate diameter and a smooth internal finish. The parts are produced using a Citizen sliding head CNC turning machine, starting from steel bar as raw materials, with tolerances on dimensions defined by the customer and limited by the turning machine tool capacity. In the honing operation, a rotating tool carrying abrasives removes minimal quantity of metal (from 0.03 to 0.3 mm) from the internal bore. The main purpose of this secondary machining operation is to finish the surface to a particular diameter with finer tolerance, smaller geometric roundness and small roughness.
The sandblasting (or shot blasting) is a mechanical cleaning process where an air jet projects individual grains of abrasive material at high speed on the parts surfaces in order to detach and remove the working burrs. The small size of the grain increases the specific pressure on the point of impact, removing the wanted layer and by reducing it in powder form. Finally, the washing is a post-machining cleaning operation to remove cutting oils, metal chips and honing residue.
Since Zannini production is divided in several stages, the final quality of the component depends upon the accumulated quality results of each individual operation, as shown in the following block diagram (see Figure 2.7).

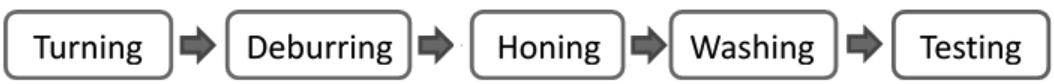

Figure 2.7: Production steps

In particular, in the GO0D MAN project the realization of a metal part for hydraulic electro valves that operates on the manual transmission of cars is considered. In Figure 2.8 two examples

of sleeves for hydraulic electro valves produced in Zannini Poland Sp.Zo.o for automotive applications like Automated Manual Transmission (AMT) systems into car transmission or Variable Camshaft Timing systems (VCT) into car engine are reported.

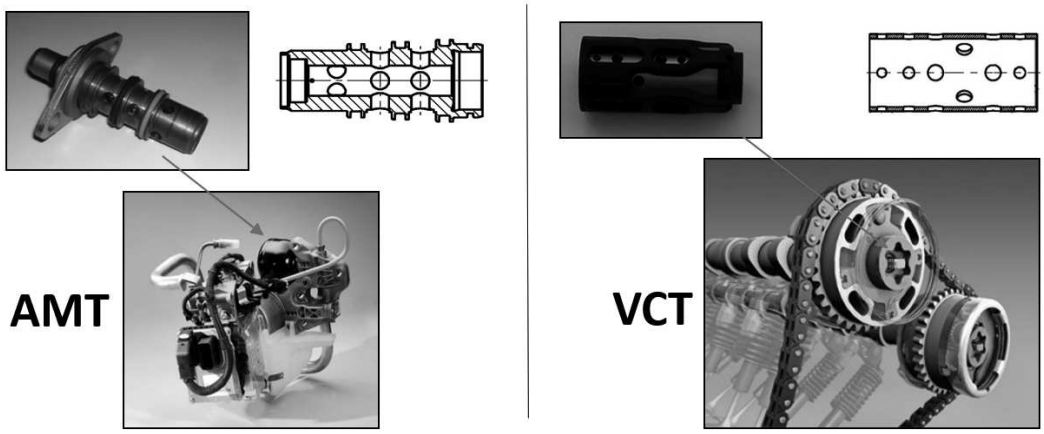

Figure 2.8: Sleeves for hydraulic electro valves for automotive applications

2.3 State of the art on quality control systems in a typical production line

Zannini has laboratories (Figure 2.9) equipped with instrumentation that includes: 3D coordinate measuring machines (CMM) using optical and contact sensors, optical profile measuring systems, Roughness and Roundness tester, Hardness tester, Technical Cleanliness tester.

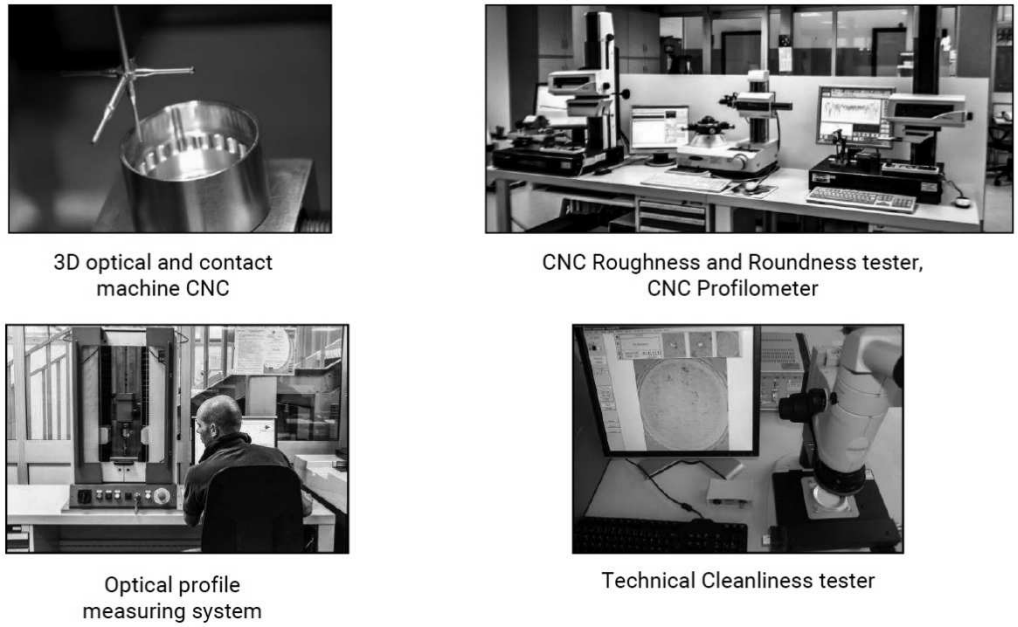

Figure 2.9: Zannini laboratory measurements equipment

On such laboratories, parts are checked at the beginning of the production in order to verify that the process has been set correctly. Measurements can be repeated on samples taken during production. During running production, the quality of the parts and stability of the process are also verified by the operator through sampling the batch according to the frequency indicated in the Control Plan (CP). The measurements are done with gauges or quality equipment available near to the production lines (see example in Figure 2.10). Measurements are recorded in the "Galileo Qualità" Quality Management System (QMS) that automatically proceeds with Statistical Process Control (SPC) analysis.

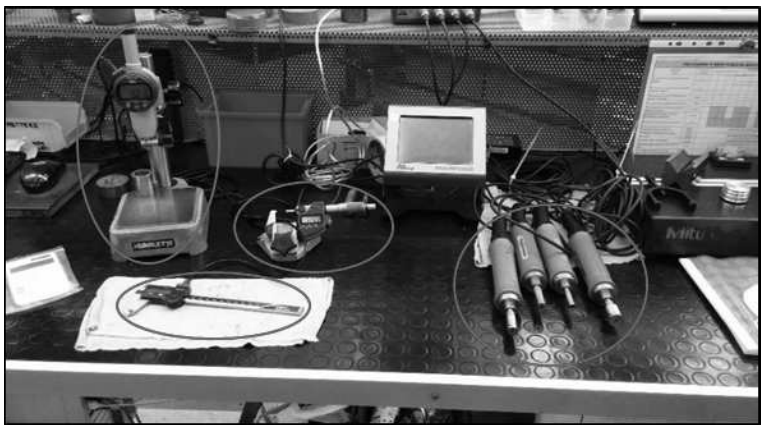

Figure 2.10: Zannini in-line measurements equipment, respectively from the left: Dial Gauge, Caliper, Micrometer, Manual Gauges

Measurements and SPC analysis results are analysed by the operators: if the dimensions and the characteristics of the products are not within tolerance, the Not OK (NOK) parts are isolated, together with all the parts produced after the last OK previous control. The same containment action is performed if the process appears to be not stable based on SPC analysis results. After the containment actions, parts potentially NOK are then verified by the Control Quality department. The department analyses the parts by using the measuring equipment of the laboratory and determine their status, then they decide if the parts can be reworked or scrapped. If the control results are positive, which means that the measured samples are within tolerance and the process is stable, the controlled parts move to the next phase of production.
Parts at the end of the production are verified by means of a final control plan. In the case of sleeves for hydraulic electro valves produced in Zannini Poland Sp.Zo.o for automotive applications, such final control plan includes a 100% final check before the parts are sent to the customer or stocked in the warehouse: NOK parts at this point are scrapped.
The product identified for testing within the GO0D MAN project is a sleeve hydraulic applications (Figure 2.11).

Figure 2.11: Sleeve to be inspected within the GO0D MAN project

The objectives of my thesis for the use case of Zannini were to develop:

1. A quality control system to automatically measure internal diameter and length in cylindrical parts by contactless technology;

2. An automated inspection system to detect the presence of burrs;

These automatic systems, replace operator based and statistical approach used before GO0D MAN implementation, the following two paragraph describes in detail the measurement of internal geometric inspection and the burrs inspection.

2.3.1 Geometrical inspection

In line quality control, to guarantee geometrical specifications, is processed manually by an operator after the turning phase. Before the GO0D MAN implementation, this check was only run as a statistical process control. In detail, the operator takes a sample and measures its internal diameters and length. In order to take these measures, the operator uses manual measurement instruments (Fig. 2.10), like manual gauges for internal diameter measurement (Fig. 2.12) and a caliper for length measurement (Fig. 2.13).

Figure 2.12: Manual gauges for internal diameter measurement.

Figure 2.13: Digital caliper for lenght measurement.

The manual gauge is made by an interchangeable gauge head, which represents the measuring element of the instrument, and by a handle, which leads the conversion and transmission of the signal. These manual gauges are able to measure the internal diameters, ovality and conicity with extreme precision but very tight tolerance (for example, with a manual gauge it is possible to measure an internal diameter between 10 and 10.02). This type of measurement, despite being accurate to one micron, presents the following problems:

- It needs to be manually taken by an operator;
- There is a correspondent manual gauge to each diameter, therefore to measure diameters of different sizes it is necessary to change the gauge head or to have more manual gauges, and this increases the costs and times to take the measurements;
- It is not possible to measure shape and internal diameters in the case of inner grooves.

Obviously the manual gauge only allows to measure the internal diameter, forcing the operator to use a different instrument (i.e. calliper) to measure the length. The system which needs to be developed must operate by the line after the turning phase, and must guarantee the automatic control over 100% of the produced pieces, overcoming the limitations of the measurement instruments used so far and allowing a more flexible and modular measurement. In chapter 3 the system that I developed for this application will be shown.

2.3.2 Burrs inspection

As reported in Figure 2.11 parts produced by Zannini have lateral holes obtained by turning machine drilling. Fluids pass through these holes and are accelerated or slowed down. During the holing phase, burrs can be produced, and these make the surface indented and not perfectly round. As a result, the desired outcome of the sleeve might change like the advance or delay of the fluid passing through them. Therefore, if burrs are present, it is necessary to remove them. As a matter of fact, deburring processes always follow the actual production. Burrs, however, are not always present and deburring processes may be unnecessary.
Currently operators carry out spot checks on the sleeves in quality laboratory. The sleeve is individually put under a light and magnifier to check if burrs are present from the inside. This type of check, despite accurate, requires the operator's expertise and it is linked to their speed of analysis. In fact, it is a repetitive process may induce human errors and hence increase the uncertainty associated to the inspection.
Since this is a visual check, it is possible to substitute it with an automatic system based on machine vision. This allows to carry out the check on all sleeves produced. The idea is to develop a system which detects burrs right after the turning phase and before the sand blasting. This type of system would allow to skip the deburring process in case burrs are not present. Also, it would allow to produce information on the honing phase and on the tool wear. The solution which I developed is aimed at imitating the operator's function automatically, thus generating a number of advantages, and is described in chapter 4.

Chapter 3

Confocal chromatic sensor quality control system for geometric feature assessment

3.1 State of the art

In regards to manufacturing of high precision components, dimensional measurements are required for conformity assessment. High accuracy data can be acquired by coordinate measurement machines (CMM) [74, 76] which may employ contact or non-contact probes. However, CMM are hardly be used inline for 100% quality control due to long inspection times and to their poor capacity to operate in harsh environments, such as production line. The use of optical sensors for dimensional measurements opens the possibility of 100% in-line quality control [28, 29] without contact. non contact measurement is important in order to ease the automation of the sensor placement and removal [21, 26], this is why the optical techniques are the best candidates. Among optical sensors [13, 10] which achieve micrometric resolution, some different options exist:

- Reflection type optical sensors (bulk optics or fiber optics);
- Laser triangulation sensors;
- Interferometric sensors.

It is difficult to develop optical probe with laser triangulation sensors or interferometric sensors with radial beam exit in the space available which is about 10mm diameter cylinder. With relevance to reflection type optical sensor a variety of measurement principles can be implemented. The most common are the intensity based reflection type and the Confocal Chromatic Sensors (CCS). The intensity based are strongly non-linear and their output can be unstable due to light source intensity drift or to variable optical absorption of the surface. For these reasons they have been excluded and we have chosen to use a confocal sensor.
Confocal Chromatic Sensors (CCS) are good candidates for measuring the internal diameter of cylindrical components. They are produced in small format and can measure in a radial direction, down to the micrometric range [43, 44].

In order to realize a measuring system for internal diameter of small components, it is necessary to select a sensor suitable to be inserted into the part and measure the radius during a complete revolution. Being the components about 10 mm diameter, the choice is really limited to few sensors. Confocal chromatic sensor was chosen for measuring internal diameter of cylindrical components with micrometric resolution. This sensor has cylindrical probes connected to a fibre optic cable [34, 37, 66, 56].
CCS measure distance at a point, which is the focal point of the sensors' front lens, using the chromatic aberration[15, 69, 53]; The confocal chromatic measurement principle was first investigated by Molesini *et al.* [49] In confocal distance measurement, a point light source is imaged onto the object while the latter is imaged onto a point detector [46, 61, 70].

The CCS exhibits the unique property of Perfect Focus Depth of Field, since at any given point of the chromatic axial field of view there is only one wavelength perfectly focused, all the other wavelengths being absolutely inactive[24]. The light is detected with a spectrometer and the measured intensity curve is spectrally coded [34, 64].

Therefore, they are single point local sensors [14]. Various authors investigated the chromatic confocal technique [68, 27, 24] and its applications for macro and microscopic analysis of surfaces [60, 41, 32, 40, 47] , and distance [59, 18, 62, 71, 23] and layer thickness measurements[48, 57, 38].

However, CCS metrological characteristics are affected by thermal disturbances which should be taken into account and compensated for [12, 35, 42, 75]. In order to reconstruct the shape of the circular section of a turned part, the sensor has to be inserted inside the cylindrical part on-axis and then accurately scanned over the part under inspection; accuracy in scanning as well as accurate alignment are fundamental for the final result. Furthermore, their use as absolute distance sensors requires specific calibration [52] and determination of the start of their measurement range.
I developed an automated quality control station based on a CCS which is rotated and scanned inside a cylinder, to measure its internal diameter.
I designed this station to be a smart QCS, I developed smart behaviours, which can compensate for some problems (self-centering of the CCS probe and temperature compensation) to reduce measurement uncertainty.

The parts to be inspected are cylindrical metal parts (Figure 2.11), with several holes drilled along their cylindrical surface. It is necessary to measure the internal diameter with an uncertainty lower than 10 μm and to measure length of the part with an uncertainty lower than 50 μm. The quality control station I developed has been therefore based on the concept of inserting axially inside the part an optical sensor capable of radial distance measurement. Then, by rotating the sensor around its axis over 360° it is possible to measure its internal diameter, while if the sensor scans it in axial direction it is possible to measure the length of the part. To implement this method, the measurement system needs to be equipped with traversing stages which can move the probe relative to the part along radial (x,y) and vertical (z) directions and rotate it around the vertical axis.

3.2 Design and realization of the measurement system: Layout and Hardware architecture

The test station which has been designed and realized (Figure 3.1) is made of four main hardware components:

1. Micrometric stages for automated motion;
2. Confocal chromatic sensor for dimensional measurements;
3. Additional temperature sensor for ambient temperature assessment;
4. Microcontroller units and Electric Cabinet.

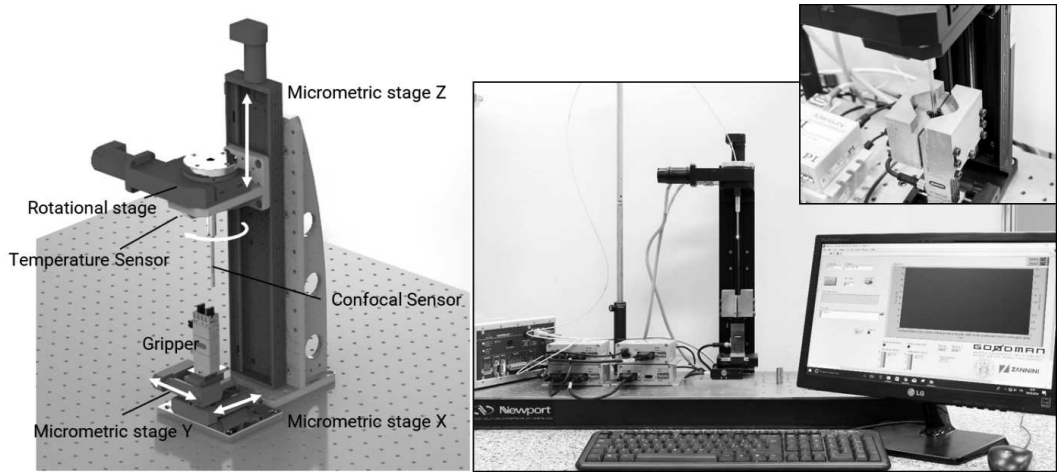

Figure 3.1: Confocal chromatic sensor quality control system for geometric feature assessment: the schematic drawing (left) and pictures of the prototype (right).

The hardware components of the test station are described in detail hereafter.

3.2.1 Micrometric stages for automated motion

In order to perform the test, the optical probe has to be first inserted axially inside the cylindrical part. This is achieved by a micrometric stage [31] which operates along the vertical z direction (axial direction), once the cylindrical part has been fixed by a clamp and positioned with its axis vertical.

Then the probe has to be rotated by 360° around its axis. This is done by a rotation stage. This rotation stage is mounted on a 90° support fixed to the z stage. The optical probe is mounted on axis of the rotation stage, i.e. with its axis vertical.

The cylindrical part is instead mounted on a gripping system, with a dovetail gripper which allows to fix the part with its axis vertical. This gripping system is mounted on two linear stages, which allow motion along x and y axis. Therefore, the part to be inspected can be moved in a plane orthogonal to the probe axis; this allows centring of the optical probe with respect to the part to be inspected.

This system architecture is designed to allow for the necessary Degree Of Freedom for the measurement and for implementing self-centring and self-calibration. These behaviours will be described in detail in the paragraphs 3.3.2 and 3.3.4

Table 3.1 reports the characteristics of the stages described above. Range, resolution and accuracy of all stages were chosen to match the requirements set for the inspection and to allow

for measurement in a large range of cylindrical parts having different dimensions (diameter and length), representative of the production of the company.

Table 3.1: Confocal chromatic sensor quality control system for geometric feature assessment: stages technical specification.

Stage	**Travel range**	**Unidirectional repeatability**
X, Y linear stages	25mm	0.1 μm
Rotational stage	>360°	175 μrad
Z linear stage	300mm	0.8 μm

Table 3.2 reports the characteristics of the electric gripping system.

Table 3.2: Confocal chromatic sensor quality control system for geometric feature assessment: technical data of the gripper EGP-25-N-N-B.

Min. gripping force $[N]$	20
Max. gripping force $[N]$	40
weight $[kg]$	0.11
Stroke per jaw $[mm]$	3
Repeat accuracy $[mm]$	$\pm$ 0.02

The gripper has the task of grasping the piece once it has been inserted between the fingers by an operator or a robotic arm and ensures its stability and maximum repeatability during grasping; in addition, it must ensure that, once the part is gripped, the part axis and the sensor axis are parallel.
The gripper has two parallel fingers which can be modified according to the type of piece to be grasped. In this specific case, I designed and made a pair of asymmetric aluminium fingers (Figure 3.2 a) with the following specification:

1. The master finger, as shown in the technical drawing (figure 3.2 b), has a v-shaped profile for correct gripping of the sleeve. When the gripper is open, the sleeve can be dropped onto the support base on this finger. furthermore, on this base there is a central opening which allows the sensor to pass over the base of the sleeve during length measurement.

2. The slave finger, as shown in the technical drawing (figure 3.2 c), has a v-shaped profile but there is no support base for the sleeve.

With these two fingers thus designed, when the piece is gripped, the forces are exchanged between the side walls of the sleeve and the side walls of the fingers, avoiding unwanted tensions on the base. This particular shape allows the piece to be centered and guarantees maximum stability and repeatability during gripping phase.

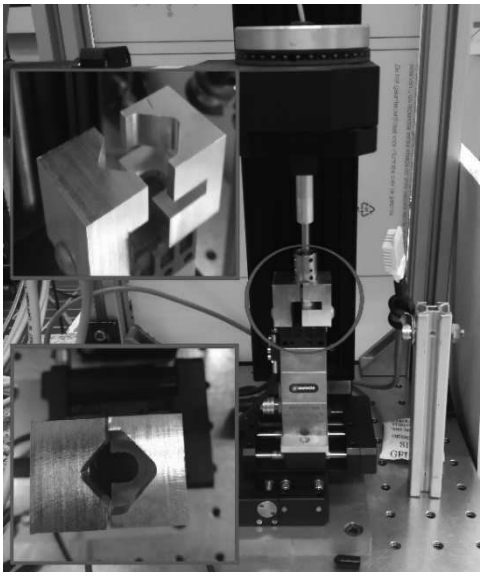

(a)

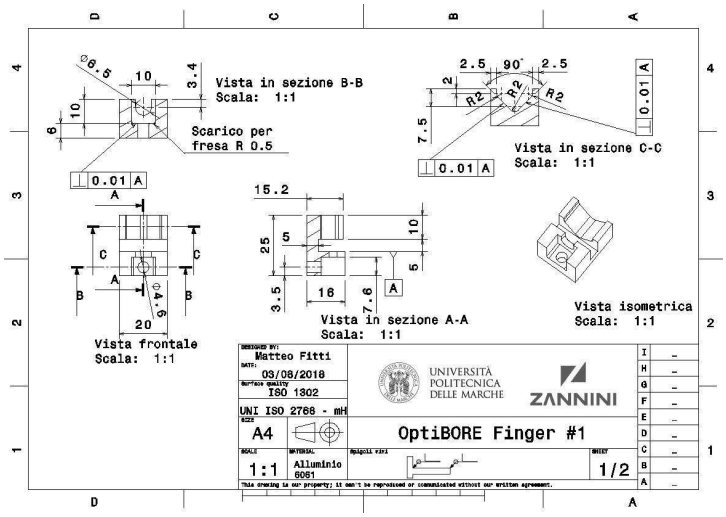

(b)

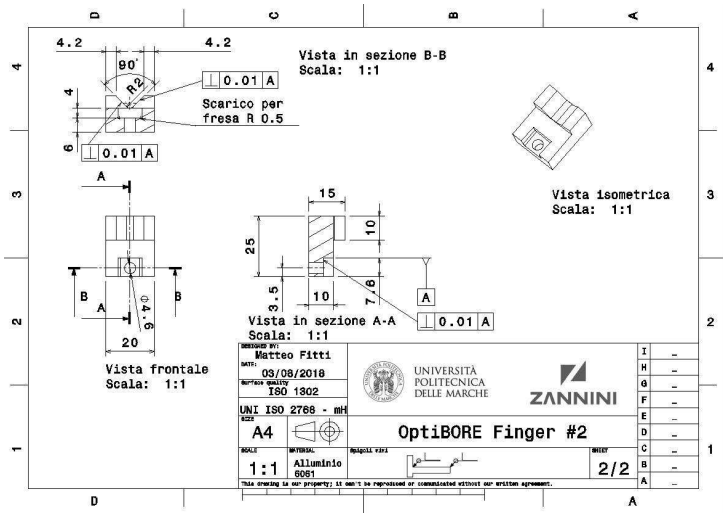

(c)

Figure 3.2: Confocal chromatic sensor quality control system for geometric feature assessment: fingers designed and used for grasping and centering the cylindrical component (a); technical drawing of the master finger (b); technical drawing of the slave finger (c).

Figure 3.3 reports the drawings of some of the mechanical parts designed to assemble the station; all parts were manufactured in aluminium. The test station is mounted on a table-top honeycomb bread-board, for assuring stability.

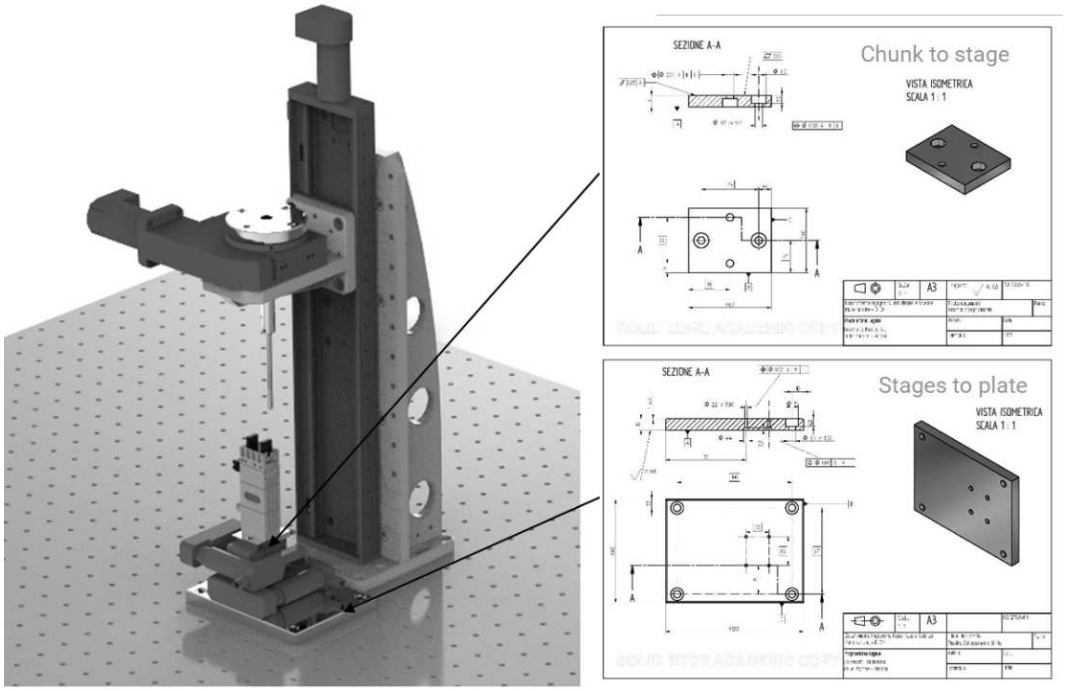

(a)

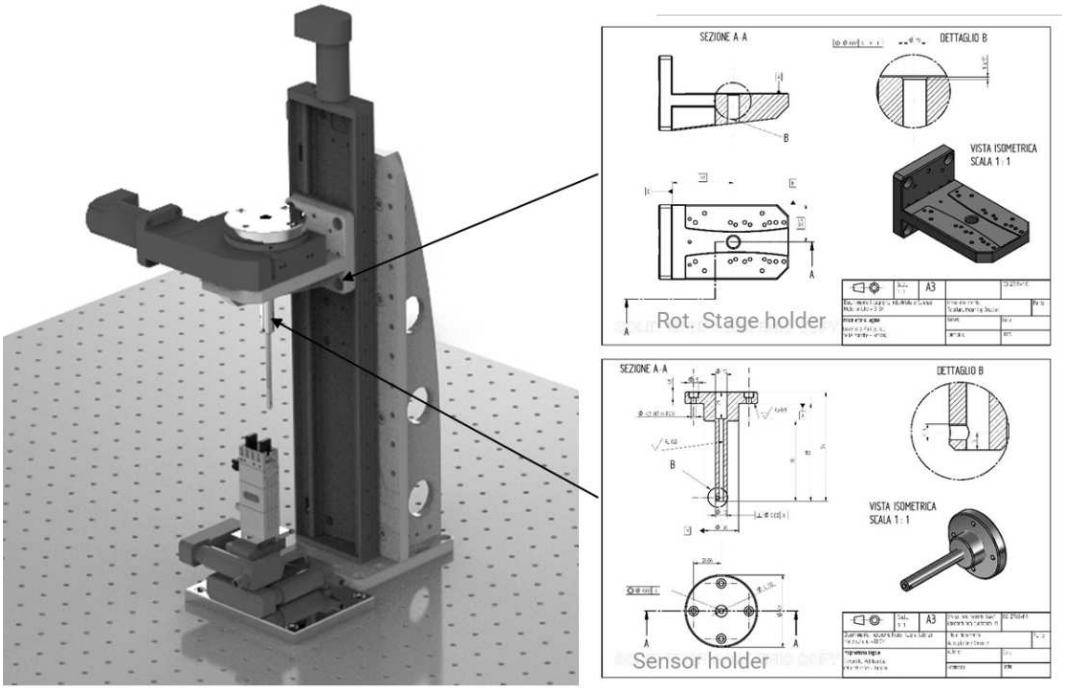

(b)

Figure 3.3: Confocal chromatic sensor quality control system for geometric feature assessment: gripper to stage coupling plate and stage to optical breadbord (a); Rotary stage holder and probe holder (b).

3.2.2 Confocal chromatic sensor for dimensional measurements

Chromatic confocal sensors (CCS - Figure 3.4) exploit chromatic dispersion lenses (lenses whose refractive index is wavelength-dependent) to measure the distance of a target in a non-contact way [63, 72]. Indeed, when a broadband light source (white light) is focused onto an object by passing through this type of lenses, only the wavelength which is effectively on-focus at the target plane will be the dominant wavelength scattered back. The backscattered light is analysed by an optical spectrophotometer, to determine which is the dominant wavelength scattered back. Changes in the measured sensor-to-target distance produce changes in the on-focus wavelength, therefore these sensors are calibrated to correlate a specific dominant wavelength with a specific sensor-to-target distance. The confocal chromatic sensor utilized is the Micro-Epsilon [6] IFS 2402/90-10 with a 90° beam exit from a 4 mm diameter probe so to make radial measurements inside small cavities and bores possible. From different manufacturers [8, 9], the one chosen is the most suitable in terms of size compared to the hole to be inspected. The sensor chosen has a range of 6.5 mm, starting from about 3.5 mm, therefore it can measure radius in the range 3.5-10 mm. Resolution is remarkably small, 0.25 μm on optically cooperating surfaces, i.e. surfaces with a diffuse scattering. On reflective surfaces the sensor performance decays, depending on the incidence angle of the light to the surface. Linearity is declared to be 13 μm. Metrological characteristics of the Micro-Epsilon IFS 2402/90-10 confocal chromatic sensor are reported in Table 3.3

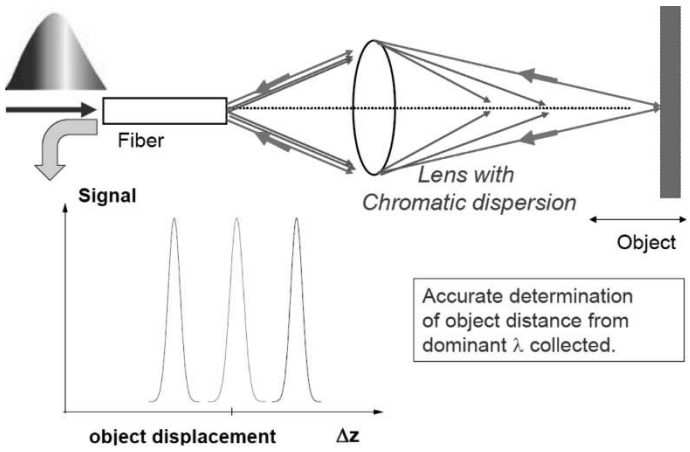

(a)

(b)

Figure 3.4: Confocal chromatic sensor quality control system for geometric feature assessment: confocal chromatic sensor for bore inspection: Measurement principle (a) [12] , Sensor used in the tool developed Microepsilon IFS 2402/90-10 (SN:7111088) (b).

Table 3.3: Confocal chromatic sensor quality control system for geometric feature assessment: Metrological characteristics of the Microepsilon IFS 2402/90-10 confocal chromatic sensor.

Measuring Range MR	6.5 mm
Linearity	13 μm $\leq \pm 0.2$ % Full Scale Output
Resolution	0.25 μm
STtart Measuring Range - SMR (Approx.)	3.5 mm
Spot diameter	100 μm
Max Tilt (direction reflection)	$\pm 1.5°$

It is important to point out that the value given by data sheet of the start of measuring range (SMR) is approximate; in fact generally these sensors are used in the measurement range (MR) to make differential measurements of distance between two surfaces or to calculate the thickness of transparent materials. To overcome this problem, a specific test methodology has been developed that allows the actual value of SMR to be measured (3.3.4).

Temperature acts as a disturbing input, because it varies the refractive index of the graded index lens used in the probe. This requires special care for applications in which the environmental temperature in not controlled (e.g. shopfloor), more details on possible strategies to compensate

for this issue are reported in paragraph 3.3.3.

3.2.3 Additional temperature sensor for ambient temperature assessment

Given the fact that temperature is a disturbing input for this quality control system, in order to allow operation in environments with varying temperature, temperature should be measured in proximity of the optical probe. For the purpose, the design includes a NTC thermistor (Figure 3.5). Measured temperature will then be used to compensate for temperature effects. Table 3.4 shows thermistor metrological characteristics.

Figure 3.5: Confocal chromatic sensor quality control system for geometric feature assessment: NTC thermistor digital sensor DHT22.

Table 3.4: Confocal chromatic sensor quality control system for geometric feature assessment: NTC thermistor characteristics.

Model	DHT22
Output signal	Digital signal via single bus
Measuring Range	-40∼80°C
Accuracy	$\leq \pm 0.5$°C
Resolution	0.1°C

3.2.4 Microcontroller units and Electric Cabinet

A microcontroller unit is used to interface the thermistor and the gripper. Figure 3.6 shows the electrical connection diagram between the microcontroller and the temperature sensor. The temperature data acquired near the confocal probe are transferred to the computer via serial USB connection.

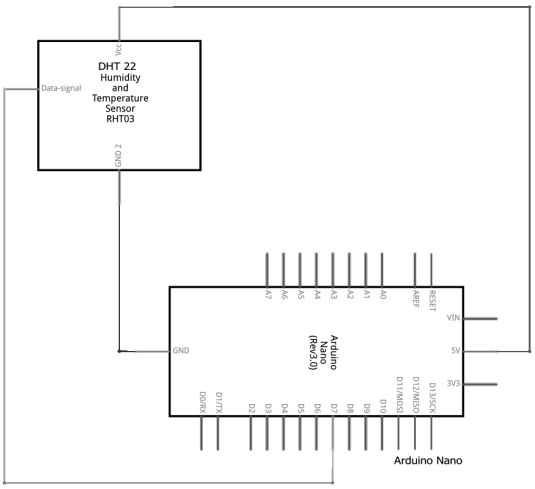

Figure 3.6: Confocal chromatic sensor quality control system for geometric feature assessment: Connection wiring of the DHT22 with microcontroller.

The second microcontroller is connected to the gripper. A double relay board connected to make it possible to control the opening and closing of the gripper. This is achieved by reversing the positive pole with the negative one on pins 2 and 4 (control pins). At the same time, by means of two proximity sensors connected to the gripper, it is possible to verify the correct opening and closing to control it in closed-loop mode. In short, the microcontroller produces the signals necessary for the opening of the gripper and reads those coming from the sensors. in figure 3.7 it is possible to observe the connection scheme of the components necessary for driving the gripper.

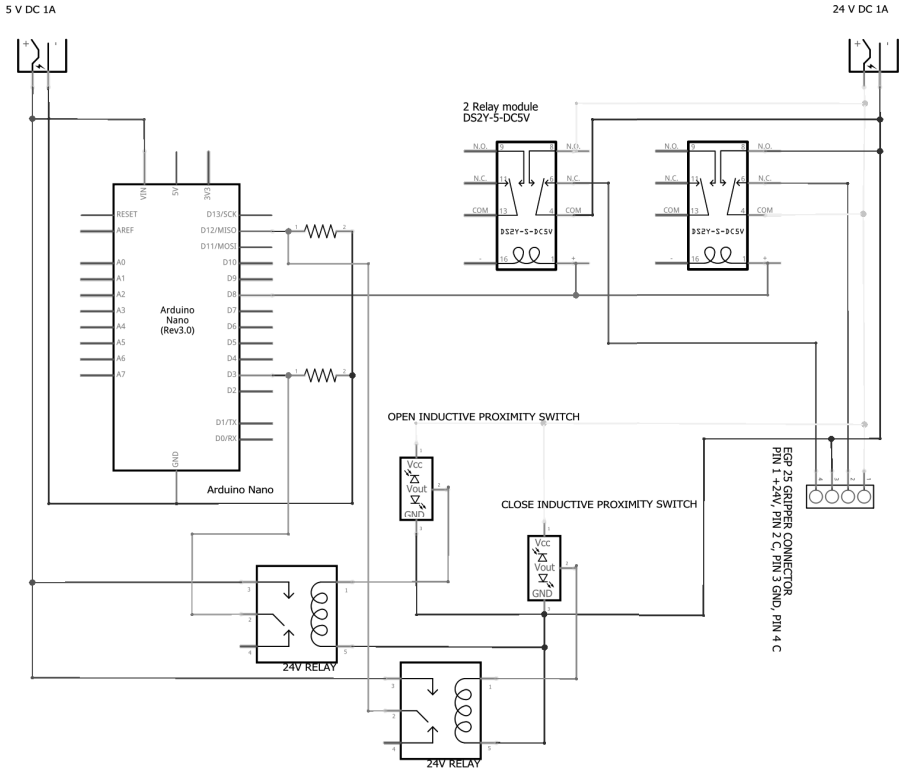

Figure 3.7: Confocal chromatic sensor quality control system for geometric feature assessment: Connection wiring for the gripper control

To ensure the proper functioning of the measuring system in the production plant, all the electronic components were arranged inside a cabinet.

Figure 3.8 shows the electric cabinet. A master switch is well evident in Figure 3.8 (b). The cabinet is provided with forced ventilation to ensure a correct temperature inside. In the lower part there are electric protection devices (magneto-thermal and differential switcher.), immediately afterwards there is a dc power supply which supplies current to all the devices, for each powered device there is a fuse protection always placed in the lower part on the right of the power supply. On the second level then there is an industrial computer that is connected to all the elements of the measurement chain and inside which the code for the measurement runs, inside the two white boxes are contained the control electronics for the measurement of temperature (Fig. 3.6) and for gripper management(Fig. 3.7). The confocal sensor controller and the four controllers of the stages connected in daisy chain are visible on the top.

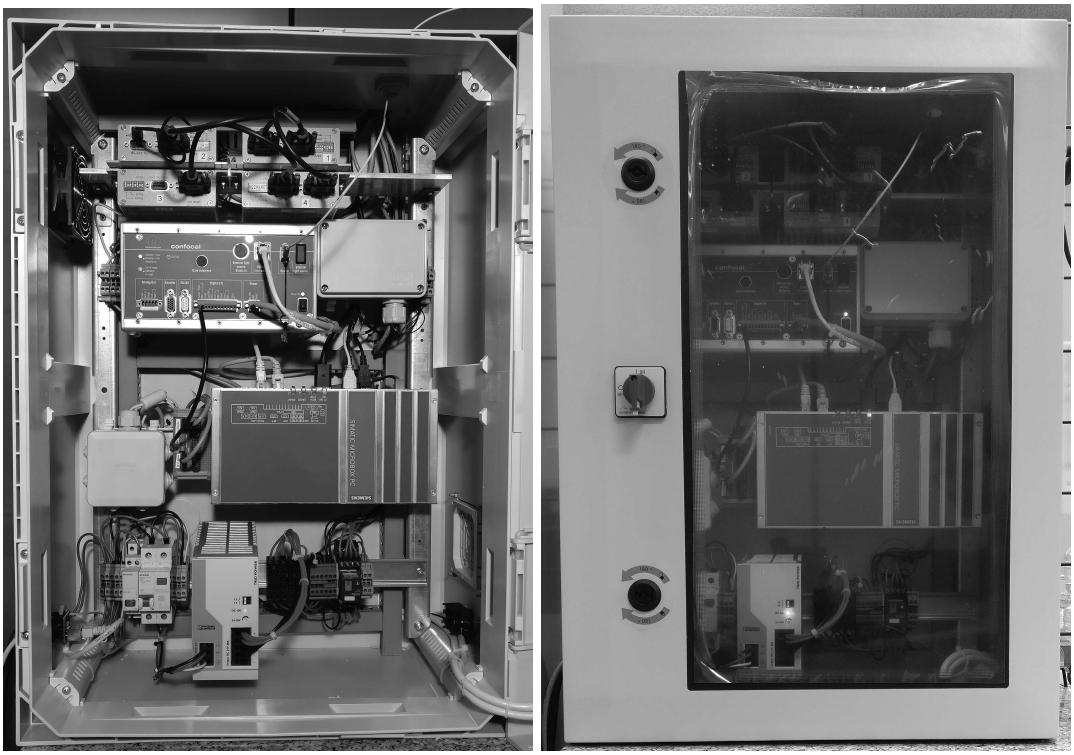

(a) (b)

Figure 3.8: Confocal chromatic sensor quality control system for geometric feature assessment: electric cabinet opened (a) and closed (b).

3.3 Design and realization of the measurement system: Smart behaviours and software

The QCS for measuring the geometrical features of cylindrical parts targets an overall uncertainty of less than/equal to 10 μm for the bore diameter. This is quite a challenge, given the in-line installation of the whole system. Indeed, it is expected, for instance, a greater variability in terms of environmental temperature with respect to a metrological room, in which temperature is highly stabilized. All these factors pushed the necessity to develop a series of smart-behaviours that could ensure accuracy and repeatability of measured data. In particular, the following three main self-adaptive behaviours have been developed for this QCS:

- Sensor-to-part centering;
- Temperature self-compensation;
- Self-calibration check.

3.3.1 Measurement procedure

The measurement procedure characterizing this QCS is illustrated in the flow chart reported in Figure 3.9. The QCS is in an idle state until it receives a trigger event (e.g. from a robot or from a software event triggered by the operator) that the cylindrical part to be inspected is ready to be measured. This event triggers a first data exchange between the QCS and its Resource Agent (RA) and the closing of the gripping system, in order to fix the position of the cylindrical part. The vertical stage carrying the Confocal Chromatic Sensor inserts the sensor axially and brings it to the section to be inspected. The correct positioning of the CCS with respect to part is then checked. If the CCS actual position is compliant with the desired position the measurement starts: data from CCS and temperature sensor are acquired during one revolution of CCS. The availability of local temperature data makes it possible to perform temperature compensation (see subsection 3.3.3 for further details) and then, through a geometric model it is possible to improve the estimation of the diameter of the section inspected. If necessary, further sections along the cylindrical part are tested. To measure the length of the part, the sensor is pulled out and taken to a certain angular sector. Taking advantage of the signal from the sensor and the position of the micrometric slides, it is possible to indirectly obtain the length of the piece, scanning it in a vertical direction along a line. Finally all these data are stored in a local database and pushed to the RA to be transmitted along the GO0D MAN architecture.

3.3.2 Sensor to part misalingnement self-compensation;

The measurement procedure requires that part axis and sensor probe axis must be coincident. In this ideal case and if the part is perfectly circular, the output signal is constant with respect to the angle. Figure 3.10 shows the three-dimensional geometry of measurement setup (top-left plot) in which blue dots represent the measurement points (only 60 in this example). The bottom plot shows the signal versus the angle and the top-right plot depicts the reconstructed geometry of the part section. This is a noise-free condition example.

A correct alignment of the sensor axis with respect to the sample longitudinal axis is of extreme importance to ensure an accurate measurement of sample inner diameter during the sensor revolution. If the axes are parallel but not coincident, the part diameter is wrongly assessed. Figure 3.11 shows the effect of misalignment between the sensor axis and the part axis that produces an eccentricity. This causes that output signal is not constant any more and the part section is incorrectly reconstructed. This effect is one of the reasons why the sensor probe is rotating in the measurement step, while is the part would be rotated and the sensor left still, one could not observe any variation in the radial distance measured. In fact, this choice makes it possible to detect the correct alignment between sensor and part axes. Moreover, also the real shape of the part under inspection can be retrieved, i.e. plastic deformation or defects, once the correct alignment is achieved.

To ensure a centering as correct as possible, the system performs a preliminary distance evaluation, at the same vertical position, on four points located every 90° along the same circumference.

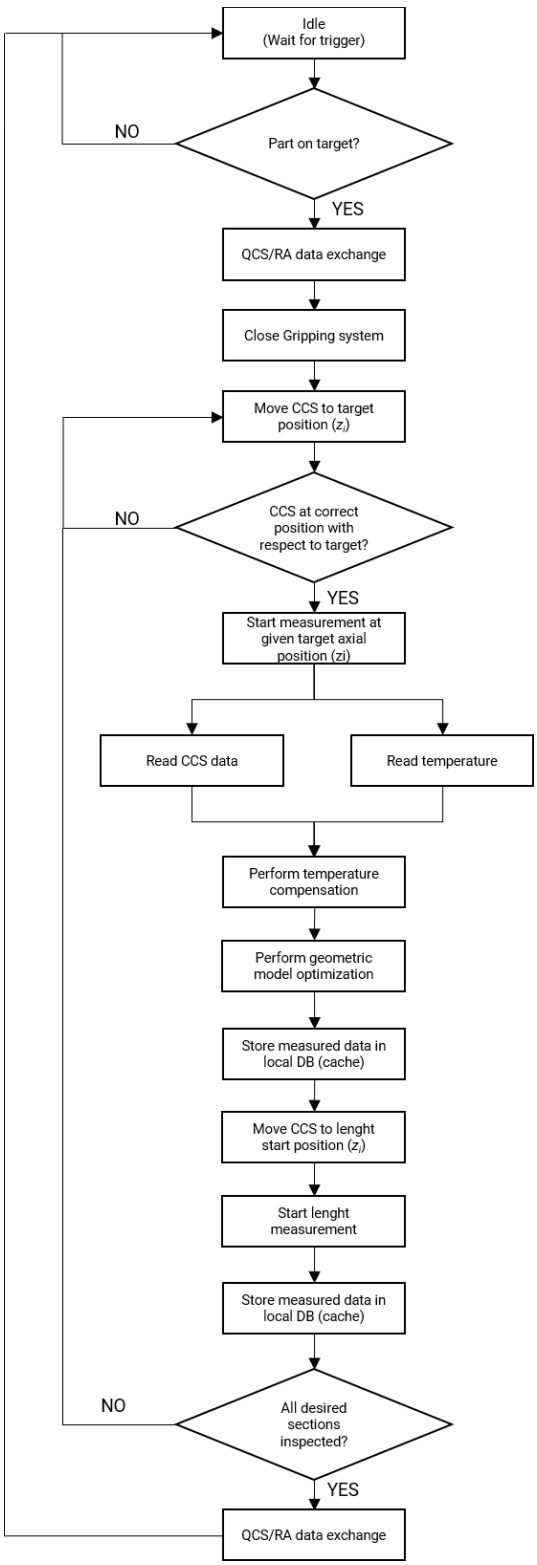

Figure 3.9: Confocal chromatic sensor quality control system for geometric feature assessment: flow chart describing the measurement procedure.

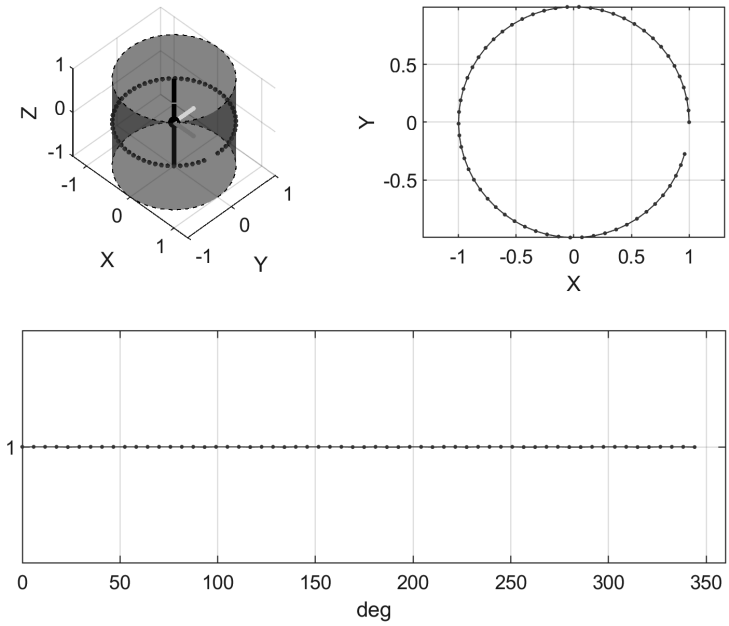

Figure 3.10: Confocal chromatic sensor quality control system for geometric feature assessment: ideal measurement condition.

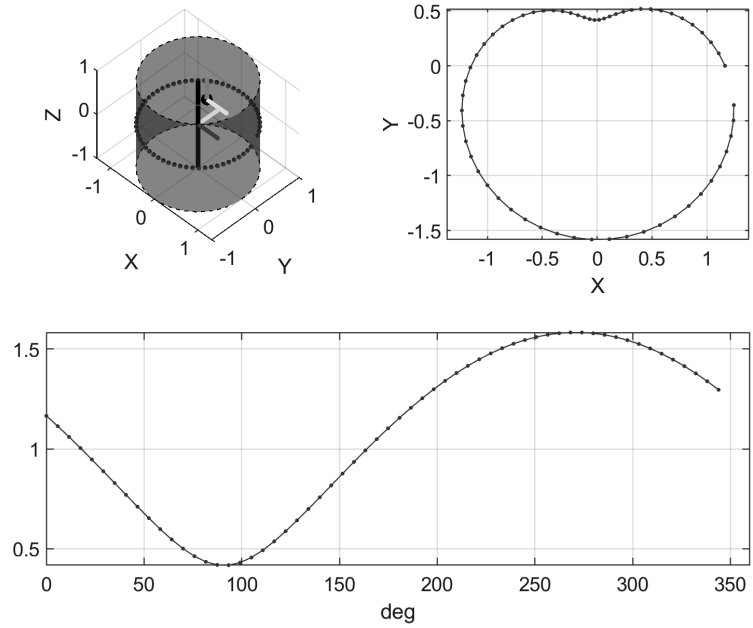

Figure 3.11: Confocal chromatic sensor quality control system for geometric feature assessment: off-center measurement condition.

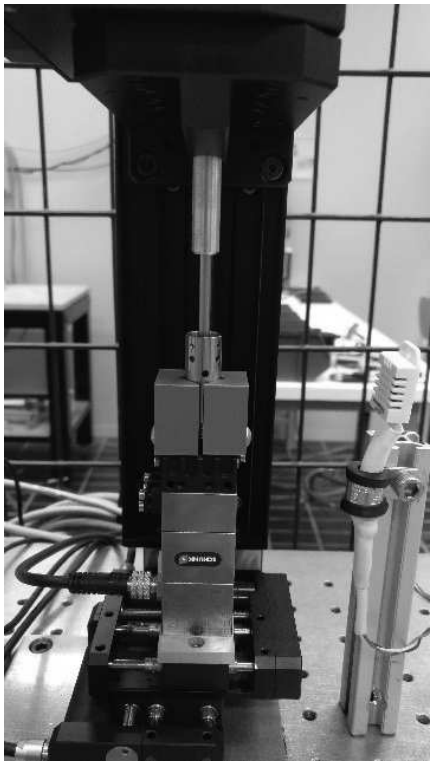

Figure 3.12: Confocal chromatic sensor quality control system for geometric feature assessment: Example of the centering operation of a sleeve.

An optimization procedure (Figure 3.12)where the sample is moved by the XY traversing axes, which means changing the relative position of the sample longitudinal axis and the sensor vertical axis, runs to make these distances equal within a certain tolerance. The centering procedure is terminated when the stop criterion is reached. After this preliminary eccentricity correction, a circle fitting is carried out and finally an analysis of residuals with respect to the circle is performed, so to refine the centering of the sensor with respect to the sample.

Figure 3.13 shows the effect of the centering operation on experimental data acquired. It is well evident that an initial deviation of approximately 0.1mm (Figure 3.13a) is exclusively due to an out of center position of the sensor with respect to the sleeve axis. During the centering operation, this deviation from the nominal value (Figure 3.13b) progressively decreases down to less than ± 10 μm.

Although, the blue line in Figure 3.13b represents the optimal centering condition, some residual deviations from the ideal curve (Figure 3.10) are present. This effect is due to non-parallel axes of sensor and part. Figure 3.14 shows the effect of incident but not parallel axes. The order of magnitude of this effect is lower of the eccentricity. In fact, the effect of tilted sensor is revealed only when the centering procedure is done.

Actually, the most likely condition in real measurement is with skew axes (not parallel and not incident axes) as depicted in Figure 3.15. By means of X and Y stages it is possible to adopt a centering procedure to make the axes coincident in the measurement section. However, the sensor axis and part axis are incident but not parallel. The relative position and orientation between sensor and part is determined by the gripping and finger systems (repeatability positioning of the part).

The maximum time requested for the inspection of each part does not allow to perform any physical axes alignment procedure. In fact, this would require measurements on multiple sections that would be time consuming. A possible solution to this problem is to consider the geometric model of measurement setup in the data processing phase. The geometric model returns the ideal measured signal given the physical parameters (part diameter, sensor eccentricity and axis direction with respect to the part). The diameter estimation can be improved minimizing the

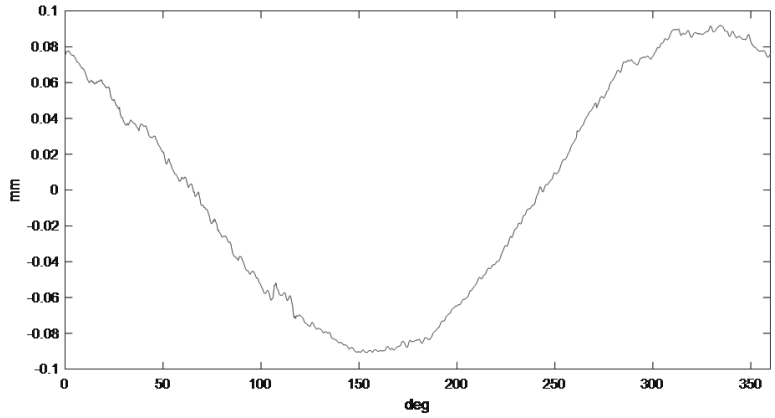

(a)

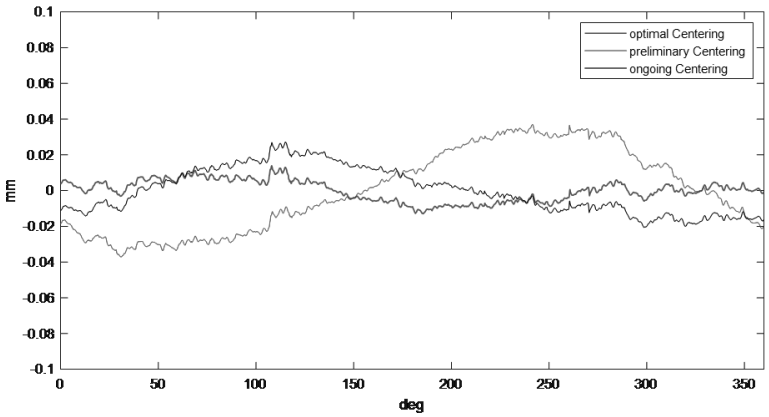

(b)

Figure 3.13: Confocal chromatic sensor quality control system for geometric feature assessment: effects of centring on measured data

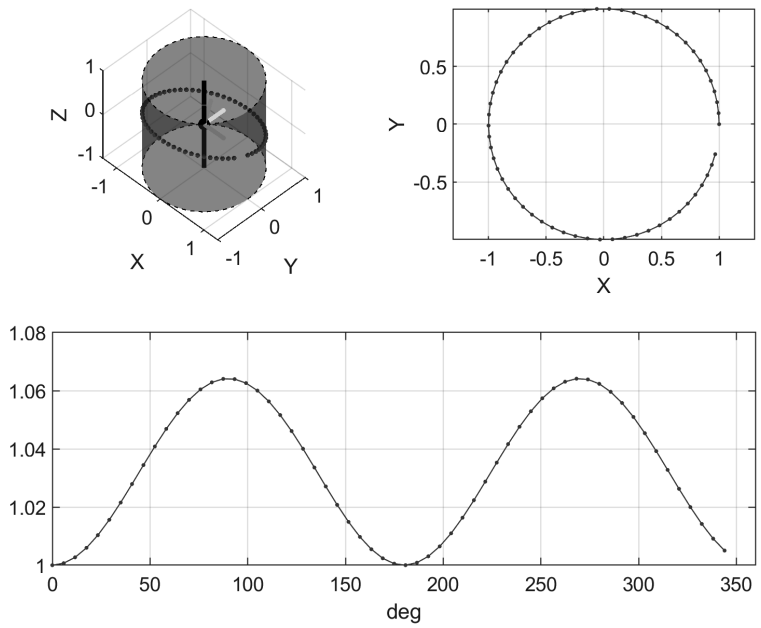

Figure 3.14: Confocal chromatic sensor quality control system for geometric feature assessment: tilt measurement condition.

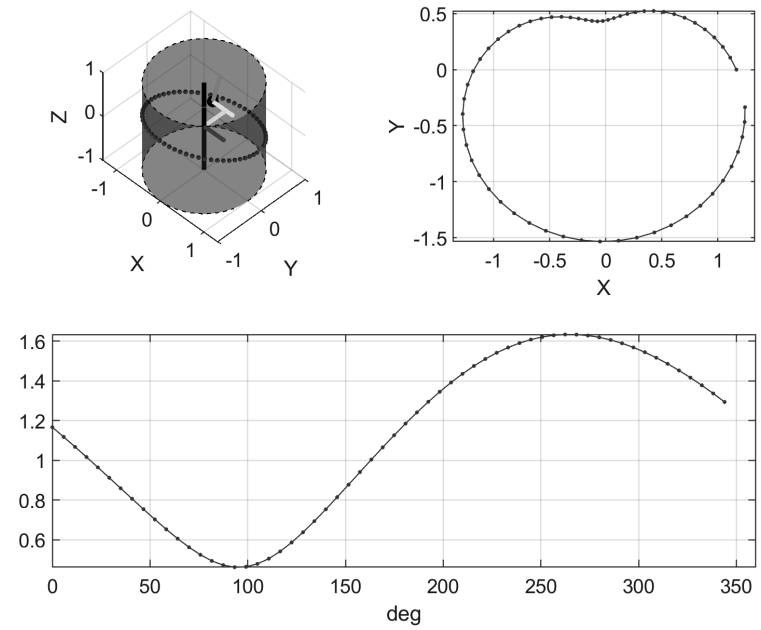

Figure 3.15: Confocal chromatic sensor quality control system for geometric feature assessment: off-center and tilt measurement condition.

quadratic difference between real and simulated signals. This procedure returns the best geometric parameters that are compatible with the measurement. Since it is a software based method, it is very fast and can be adopted for each part. This is the reason why it has been adopted in the measurement process.

3.3.3 Temperature self-compensation.

Ambient temperature represents a modifying effect for the chromatic confocal sensor and therefore it is necessary to compensate the erroneous distance value provided by the sensor [12]. Indeed, temperature variations causes a twofold effect on the CCS, i.e.:

- Onset of spurious displacement Δz

$$n(\lambda_0, T_0) = n(\lambda_0 + \Delta\lambda, T_0 + \Delta T) \tag{3.1}$$

$$\Delta\lambda = -\Delta T \cdot \left(\frac{\partial n}{\partial T} / \frac{\partial n}{\partial \lambda} \right) \tag{3.2}$$

$$\Delta z = -\Delta\lambda \left(\frac{z_{max} - z_{min}}{B} \right) \tag{3.3}$$

where n is the refraction index of the optics, λ_0 is the dominant wavelength recorded for an object at distance z at the standard temperature T_0 and B is the source bandwidth.

- Variation of sensor working range $|dz_{max} - dz_{min}|$:

$$dz_{min} = \frac{y^2}{(y - f_{min})^2}, dz_{max} = \frac{y^2}{(y - f_{max})^2} \tag{3.4}$$

where f represents the effective focal length of the optics, and y stands for the distance (fixed) from the confocal fiber tip to the optics.
A natural consequence is that the working range increases while decreasing temperature and the sensor undergoes temperature drift. A dedicated measurement campaign was performed to experimentally characterize the correlation between ambient temperature and measured distance. The CCS was installed inside a temperature controlled chamber, together with a reference micrometer, arranged in a way to measure the distance to the moving plate of the micrometer (Figure 11). Since it is expected that temperature variations cause different effects at different sensor-to-target distances (z), the measurement campaign consisted in measuring five different sensor-to-target distances at different temperatures (Figure 11). The nominal distances (D_n) were evaluated by the micrometer, whose readout was also monitored by a custom-made vision-based system. The temperature range investigated ranged between 10°C and 40°C.

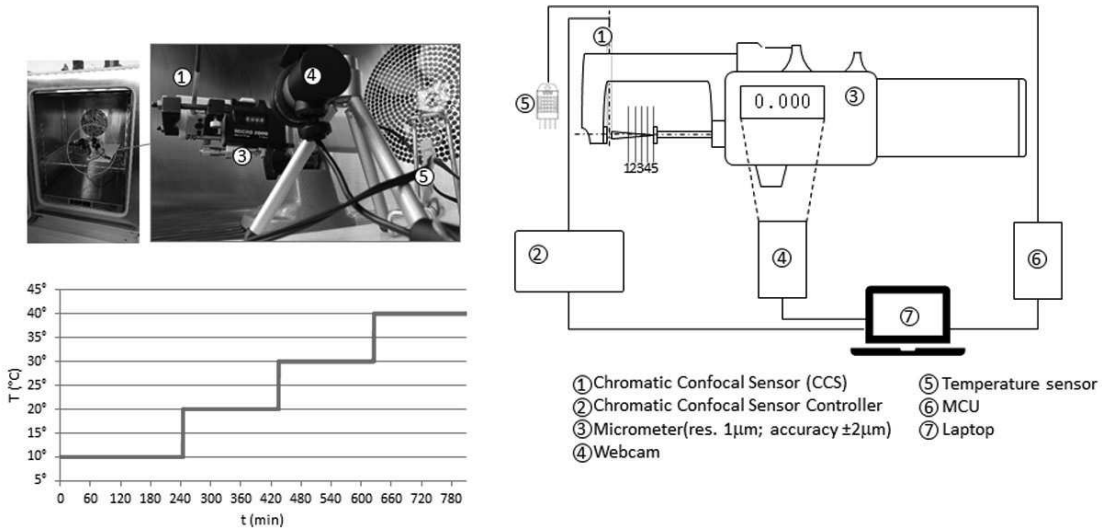

Figure 3.16: Confocal chromatic sensor quality control system for geometric feature assessment: Test setup for temperature compensation - arrangement of the monitoring set-up (top-left), measurement chain (top-right) and temperature ranges investigated (bottom-left).

Data obtained made it possible to characterize the temperature drift of the sensor. Figure 3.17 shows the dependence of the CCS sensor readout (d) vs. the ambient temperature (T). It is interesting to notice that an average drift of approximately 8 μm/°C characterizes the CCS used in the test.

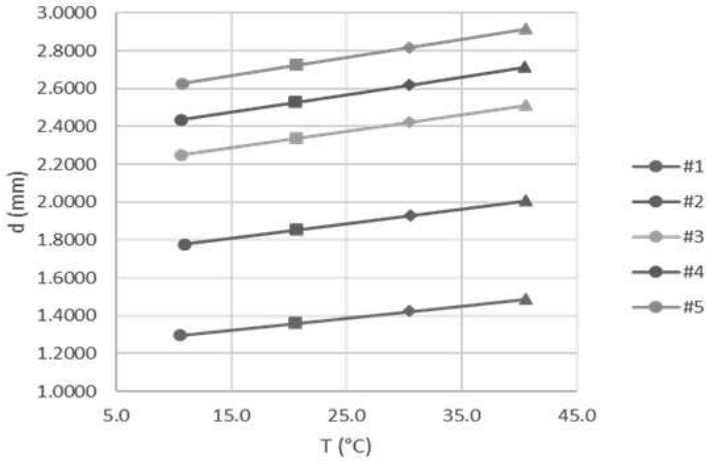

Figure 3.17: Confocal chromatic sensor quality control system for geometric feature assessment: CCS readout (d) vs. ambient temperature (T) at different sensor-to-target nominal distances.

Figure 3.18 shows the relation between the nominal sensor-to-target distances (D_v) and the CCS readout at different ambient temperatures. The decrease of the slope of the interpolating line with an increase in temperature is a further proof that the CCS working range (WR) is decreasing.

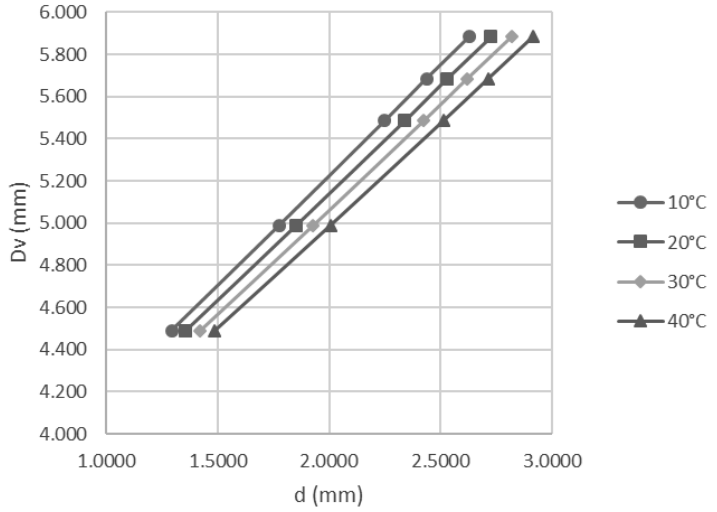

Figure 3.18: Confocal chromatic sensor quality control system for geometric feature assessment: Nominal sensor-to-target distance (D_v) vs. CCS readout (d) at different ambient temperatures.

The average temperature drift of the sensor was estimated in approximately 8 μm/°C.
By exploiting a surface fitting of the data collected during the tests (Figure 3.19), it was possible to get the sensor-to-target distance value (D_v) given the distance value (d) provided by the sensor and the ambient temperature (T) measured close to the sensor. This allows temperature compensation.

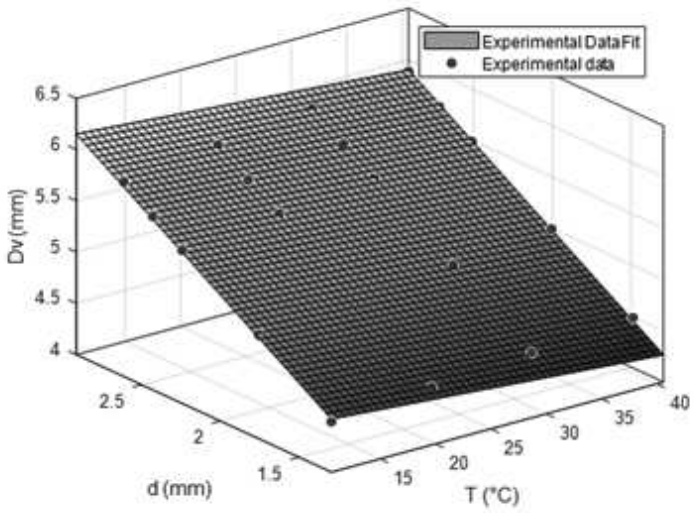

Figure 3.19: Confocal chromatic sensor quality control system for geometric feature assessment: Surface fitting to extract absolute sensor-to-distance values (D_v) given sensor readings (d) and ambient temperature (T) values.

Effects of temperature compensation on measured data are reported in Figure 19. Here, temperature offsets data (blue curve), is creating false deviations from nominal values. On the contrary, once temperature is compensated by exploiting the procedure described in Section (black curve), deviations are highly limited and residuals refer to deviation with respect to circular shape.

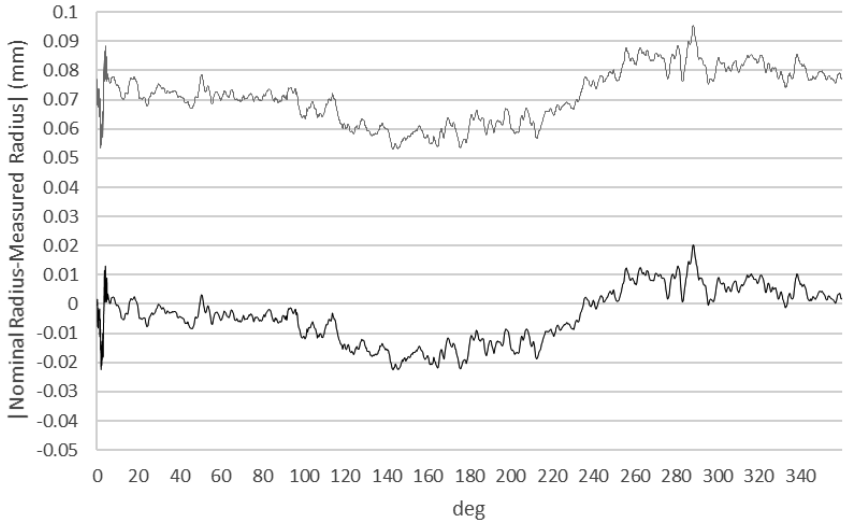

Figure 3.20: Confocal chromatic sensor quality control system for geometric feature assessment: effects of temperature compensation on measured data – not compensated data (blue curve) vs compensated data (black curve).

The average diameter value on the section scanned differs 0.001mm with respect to the one measured with a CMM. This value is negligible for our application. The standard deviation was evaluated assuming data acquired over a whole rotation as constituting the statistical population, a standard deviation of 0.009mm has been measured.This value is compatible with the nominal expected diameter of the reference sample at that section height, thus proving that the QCS, by exploiting its smart capabilities, i.e. self-centering and temperature self-compensation, is able to provide highly accurate dimensional data.

3.3.4 Self-calibration check.

It is important to periodically check the performance of the system so to ensure an uncertainty lower than 10 μm; indeed, dimensional measurements at this level of uncertainty are subject to many disturbances [51]. Periodic check has therefore to be implemented by testing the correctness of both the temperature compensation and the self-centering approaches through the sequence of operations reported in the flow diagram of Fig. 3.21. In case any of the two steps fail, it becomes possible to perform eventual interventions on the system (e.g. check of the screwing torques of mechanical parts) so to bring back performance at the desired levels.

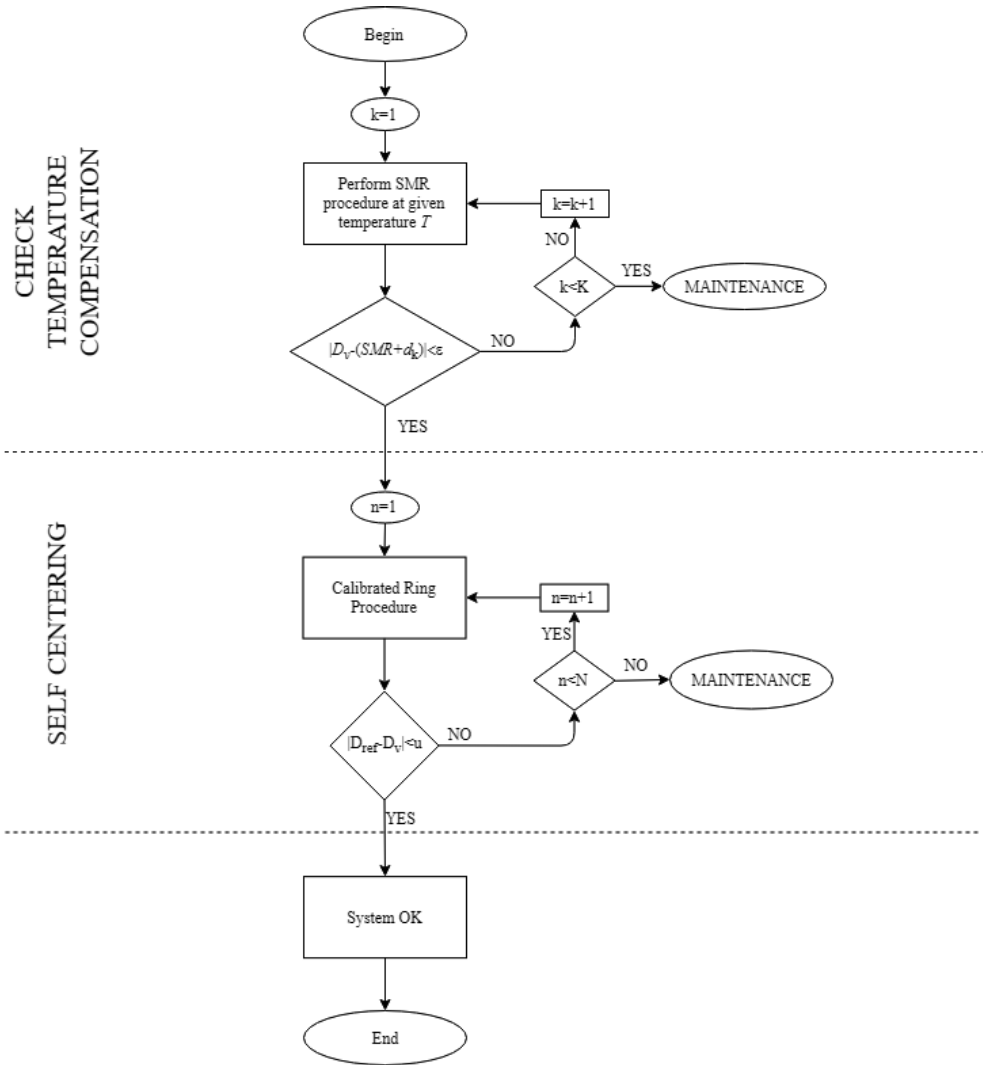

Figure 3.21: Confocal chromatic sensor quality control system for geometric feature assessment: Self-calibration check procedure.

The Start of Measuring Range (SMR) value at a known temperature can be calculated by running a dedicated two-steps procedure (Fig. 3.22) in which the sensor-to-target distance (d_1) is evaluated on the opposite sides of a target of known thickness (b) after moving the target by a known displacement value (A) (e.g. by exploiting micrometric stages). A reference gauge block (thickness accurate up to micrometric values) can be exploited for the purpose. The SMR can then be extracted using Eq. 3.5:

$$SMR = \frac{A - b - d_1 - d_2}{2} \tag{3.5}$$

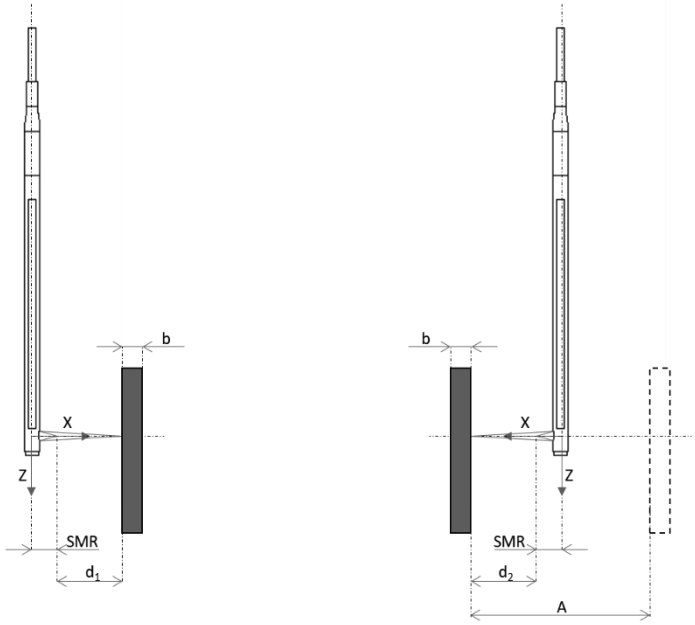

Figure 3.22: Confocal chromatic sensor quality control system for geometric feature assessment: SMR evaluation procedure: (i) sensor-to-target distance measured on the first side of the reference target of known thickness (left); (ii) target moved by a known displacement value (A) and sensor-to-target distance measured on the opposite side of the target (right) with respect to (i).

The SMR value thus obtained is used to test the validity of the temperature compensation procedure. If data extracted by the distance-temperature fitting (D_v) differs from the absolute value obtained as the summation of the SMR and the distance value provided by the sensor at k^{th} step by more than a fixed threshold ε, the procedure has to be repeated until a maximum iteration number is reached. If the latter condition takes place, a maintenance operation is performed.

In case the temperature compensation procedure succeeds, the efficacy of the self-centering approach is checked. To do so, a calibrated reference ring (micrometric accuracy) has to be used. The known radius value of the calibrated ring is compared to the radius estimated through the confocal sensor. If these two radii differ more than the target uncertainty, the self-centering procedure has to be repeated. This process iterates until either the former condition is verified or a maximum number of iteration (N) is reached. If the self-centering verification process stops because the maximum number of iterations is reached, a maintenance operation has to be performed, otherwise the whole system is intended to be verified up to the desired uncertainty.

3.4 Metrological performance: Laboratory tests

In order to evaluate the metrological performance of the system in different operating configurations, so as to be able to identify the best performing one, specific repeatability and reproducibility tests were performed on different samples in laboratory condition (Fig. 3.23).
What we want to highlight with the repeatability tests is the effect of the single instrument in the measurement uncertainty; in fact the simple instrument presents a profoundly complex nature in itself, and is affected by an infinity of small errors of different nature that combined together give rise to random errors. The uncertainty value determined with the repeatability tests represents the lower limit of uncertainty associated with the instrument.

The component under examination was grasped by the gripper and removed only at the end of the test campaign. Once grasped, the gripper was no longer moved and the same measurements were made repeatedly over it.
The reproducibility tests were carried out by repeating the measurement of the same component in conditions closer to the real operating conditions, thus introducing the uncertainty due to the gripping system. The uncertainty calculated with the reproducibility tests will be the one that actually characterizes the measurement system as a whole and on its value it is possible to verify the compliance of the system performances with respect to the specifications and design for the required dimensional tolerances.

Figure 3.23: Confocal chromatic sensor quality control system for geometric feature assessment: laboratory measurement setup.

The settings of the measurement system in the execution of repeatability and reproducibility tests are the following:

- For the rotational stage a scanning speed of 40deg/s with a step triggering of 0.1deg (with triggering type "Edge Triggering measuring value input");
- For the vertical stage a scanning speed of 20mm/s with a step triggering of 0.01 mm (with triggering type "Edge Triggering measuring value input");
- For X and Y stages used for centering the sensor on the component a speed of 2mm/s;
- For the confocal sensor a sampling frequency of 10kHz.

for each measurement cycle, a scan is acquired on a circumference in the middle section of the part to know the internal diameter and a scan along a vertical line to measure its length (Figure 3.24).

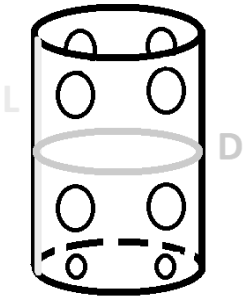

Figure 3.24: Confocal chromatic sensor quality control system for geometric feature assessment: Lines scanned on the component at each measurement cycle (D and L).

The sensor was centered on the component once a day before starting the tests, after which the X and Y slides were no longer moved during the measurements.
The parameters changed during the tests are listed below. These parameters influence the measurement uncertainty. Seven parameters were changed and twenty three types of tests were carried out by randomly combining the presence of them.

1. Rubber surface on the finger base. The fingers of the gripper have an internal V-shaped profiles, when the piece is gripped, the forces are exchanged between the side walls of the sleeve and the side walls of the fingers, avoiding unwanted tensions on the base. However, a rubber surface on the base of the Master finger (in Figure 3.25 is highlighted) prevents any tension that can occur if the piece is not positioned well, sin order to reduce the uncertainty on the gripping mode.

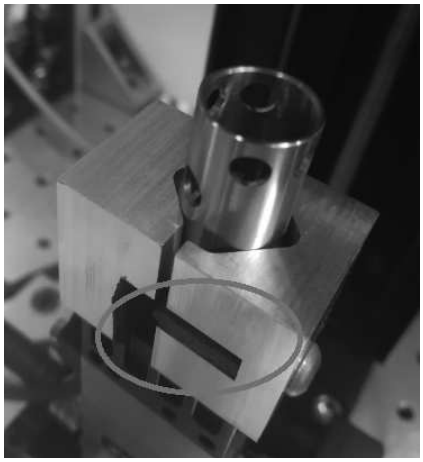

Figure 3.25: Confocal chromatic sensor quality control system for geometric feature assessment: rubber surface on the finger base.

2. Gripping force regulation. With the support of a simplified 2D fem, it has been estimated the effect of the maximum gripping force of the clamp (40N) on the component. It has shown that this force determines displacements and deformations on the piece that are substantially negligible in the order of 0.101 μm (Figure 3.26). However, a greater gripping force probably allows a more firm grip of the component but, on the other hand, given the electrical nature of the feeding of the clamps, the higher current that flows causes their overheating. Tests were then conducted by adjusting the grasping force to 100% of its potential (40N) and others to 50% to assess the best strength setting.

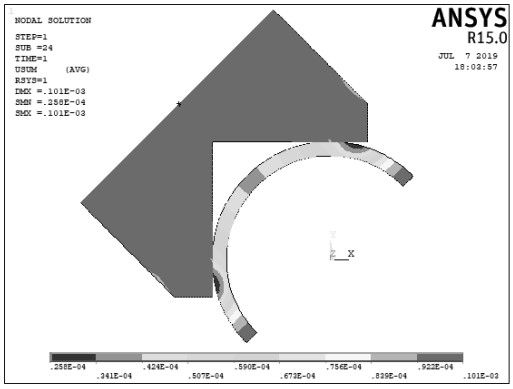

Figure 3.26: Confocal chromatic sensor quality control system for geometric feature assessment: 2D model simulation with 40N force.

3. Waiting time between one measurement cycle and the next. Some tests were performed without waiting for time between two consecutive measurement cycles, while others were performed waiting 30 ±5s between one cycle and the next so as to provide a longer time for the eventual dissipation of the heat coming from the electric motors and thus limit possible system overheating.

4. Additional auxiliary cooling system with forced ventilation positioned at the top of the system.

In addition to the cooling in the electric cabinet (Figure 3.27, indication A), an additional fan was inserted at the top of the system that pushes air from top to bottom (see Figure 3.27, indication B) to limit any thermal gradients in the area where the CCS sensor operates and where the DHT22 thermal compensation sensor is located.

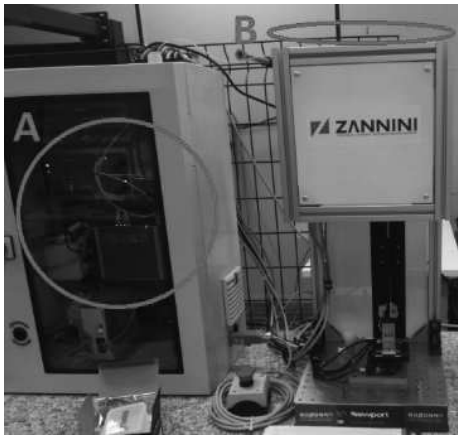

Figure 3.27: Confocal chromatic sensor quality control system for geometric feature assessment: fan cooling systems.

5. Change in the positioning of the temperature sensor. The positioning configurations "A" and "B" have been compared (see Figure 3.28) which differ in the fact that the configuration "A" is much closer to the working area of the confocal sensor.

Figure 3.28: Confocal chromatic sensor quality control system for geometric feature assessment: change in the positioning of the temperature sensor.

The configuration that produces a lower standard deviation for the diameter and length measurements is characterized by the following parameters:

- The gripper's clamping force is 20 N;
- The position of the temperature sensor is near the CCS probe;
- There is the presence of the cooling fan inserted at the top of the system;
- There is the presence of the support rubber.

3.4.1 Estimation of measurement uncertainty in laboratory condition

It is of fundamental importance to provide the uncertainty associated with the measured value. The uncertainty is therefore an index that indicates the total variability of the measurement results; the reason why the measured magnitude fluctuates around the nominal one is due to the presence of interfering inputs (random or systematic) or modifiers that produce random and / or systematic errors.
These interfering and modifying inputs can be corrected but nevertheless we arrive at a point where it is no longer easy to understand and correct these unwanted inputs and we will have a measure affected by a variability due to random errors that determine the amplitude of measurement uncertainty.

The evaluation of the uncertainty of an instrument, according to the Guide to Expression of Uncertainty in Measurement (GUM) [30] regulation, can be done by following two possible paths that go under the name of category A and category B uncertainty.
Category A uncertainty is based on statistical methodological approaches; it therefore consists in examining a certain statistical sample representative of the condition and final configuration adopted of the operation of the instrument in real operating conditions and therefore subject to all the possible real factors that influence the measurement.
In the specific case, the value of the uncertainty was evaluated considering the final setting chosen, ie the one with the test setting settings that was ranked first in the analysis and search for the best compromise setup.
From the dataset of diameter and length measurements it is possible to derive the statistical distribution calculating the standard deviation, from which with a coverage factor k=2, the expanded uncertainty (Type A) is obtained:

$$u_D = \pm 2\sigma_D \cong \pm 6 \times 10^{-3} mm$$

$$u_L = \pm 2\sigma_L \cong \pm 2.5 \times 10^{-2} mm$$

where u_D represents the uncertainty for the diameter measurement and u_L represents the uncertainty for the length measurement (of the entire measurement system). This confidence interval allows us to say that at 95% the value of the measurand will fall within this band.

3.5 Results in a real production line

The system is located right at the exit of the turning machine (Figure 3.29). Parts delivered by the machine are picked by the robot, which provides to the removal of oil film still covering the part to be inspected. After cleaning operation, the part is inserted in a holder carrying two pencil probes targeted to the measurement of external diameter(Figure 3.30 b). After this operation is done, the robot removes the part from the pencil probes holder and place it in the gripper of the Confocal Sensor station (Figure 3.30 c). At this stage, internal diameter and overall part length are assessed. After inspection is done, and depending on the inspection overall result, the part is automatically placed among good parts or scraps by the robot. A dedicated HMI reports inspection results, as well as historical trends and raw signals from the Confocal Sensor. In fact, all data measured at the station are stored in a local database and sent to the MAS system.

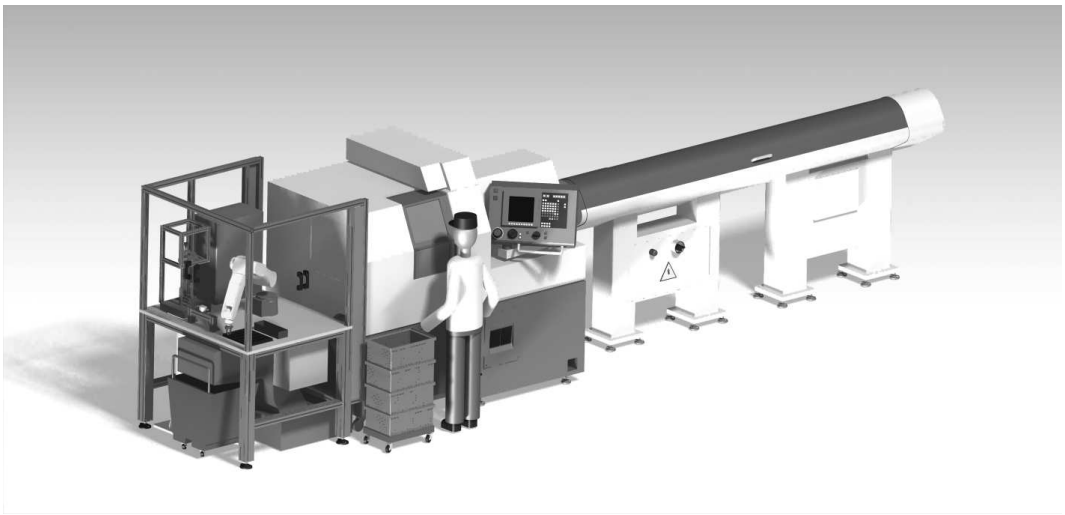

Figure 3.29: Confocal chromatic sensor quality control system for geometric feature assessment: 3D rendering of the turning machine with the geometrical feature inspection system.

Unfortunately the rotational stage enabling the measurement of the internal diameter stopped working (mechanical failure) at the beginning of August, thus making impossible the measurement of this geometric quantity.
Since it was not possible to replace the broken stage in a short time frame, it was agreed to skip the measurement of internal diameter and keep the external diameter and length measurement active. Internal diameter data to be considered for production process analysis are those acquired during the monitoring period 24/06/2019 - 01/08/2019.
Figure 3.31 shows the distribution of Internal Diameter values for the monitoring period 24/06/2019 - 01/08/2019. The dataset is composed of 15470 parts. An average value of 10.967 mm is to be reported. This is quite well aligned to the Di nominal value of 10.97 mm. The expanded uncertainty associated to the measurement, calculated as Type A uncertainty in laboratory tests, is ± 0.006 mm (coverage factor 2). The standard deviation reported from in-line measurement right after the turning operation is 0.017 mm, which is three times higher than the uncertainty of the measurement and causes a confidence level of 0.034 mm (95%). Nevertheless, the Di data show a higher spread than recorded in laboratory conditions. This can be due to the lower Signal to Noise Ratio (SNR) provided by the oil film layer, as well as burrs due to the turning process, still present on the internal surface despite the compressed-air cleaning step.

(a)

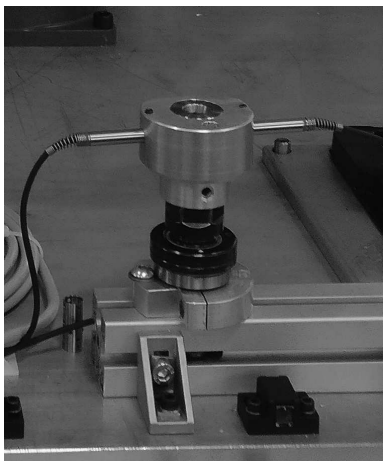

(b)

(c)

Figure 3.30: Confocal chromatic sensor quality control system for geometric feature assessment: Overview of the whole system for dimensional measurements (a); close-up on the external diameter (b) and inner diameter + length (b) check stages.

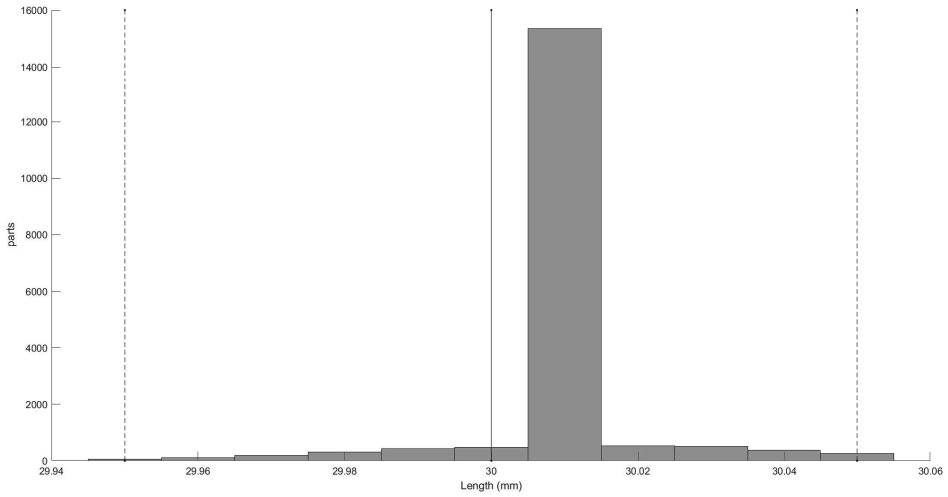

Figure 3.32: Confocal chromatic sensor quality control system for geometric feature assessment: Length analysis for the two monitoring periods 24/06/2019 - 01/08/2019 and 7/08/2019 - 23/08/2019. Bin width is 0.01 mm; nominal L value is depicted as solid black line; lower and upper boundaries are reported as dashed black lines.

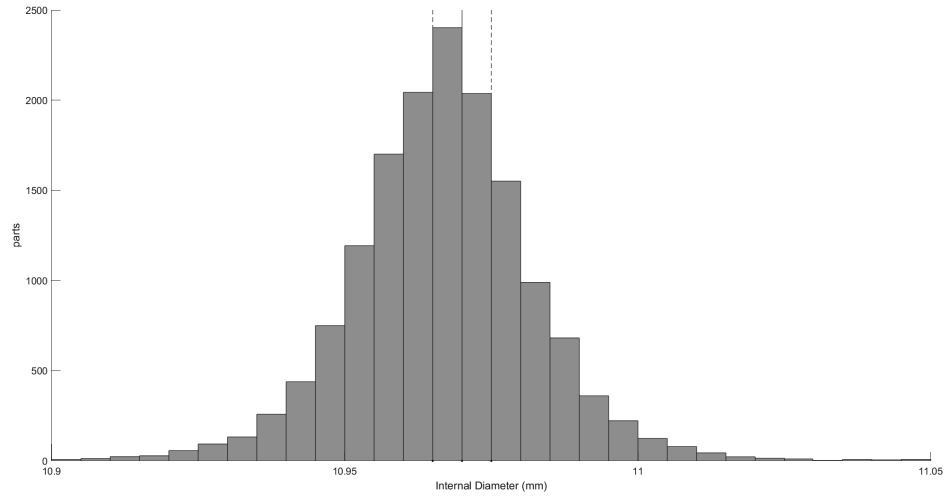

Figure 3.31: Confocal chromatic sensor quality control system for geometric feature assessment: Internal diameter analysis for the monitoring period 24/06/2019 - 01/08/2019. Bin width is 0.005 mm; nominal Di value is depicted as solid black line; lower and upper boundaries are reported as dashed black lines.

The acceptability range for Di is 10.97 ±0.005 mm. Given the distribution above, only 28.9 % turned out to be compliant with design constraint.
Figure 3.32 shows the distribution of length data over a population of 19527 parts (union of parts from the two monitoring periods). Design constraints on the length are 30.00 ±0.05 mm. Resolution of the system for measuring length is 0.01 mm. Data measured shows the highest frequency at 30.01 mm with a bin width of 0.01 mm. The confidence level for the dataset is to be estimated in 0.28 mm (95%), this demonstrating the stability of the process in terms of turned parts' length.

Chapter 4

Quality control system for burrs identification

4.1 State of the art

Several industrial sectors make extensive use of high precision turned components. Functionality of these components is strictly related to geometric tolerance. Such parts are produced in batches, often in several thousand sequences.
Concerning manufacturing of high precision turned components, dimensional measurements are required for conformity assessment; for this purpose quality control takes place either on a sample based procedures, which exploits specific instruments in the metrologic laboratory of the plant, or on 100% production, by in-line measurement equipment, at the cost of lower metrologic performance [19, 20]. At the same time, a proper working condition of these turned parts can be achieved if no burrs are present in the functional holes, i.e. the transversal holes on the cylinder.
Therefore, it is of extreme importance to detect the presence of burrs: indeed, the part can be either re-worked, whenever it is possible, or can be rejected, but no parts non-compliant to functional standards are released to the end-user. Therefore in-line quality control on 100% of production is now becoming mandatory, in the perspective of ZDM.
Burrs are metal pieces approximately 1 mm long and 0.05-0.10 mm thick created during machining process [[36]]. Fig. 4.1 (left) shows typical burrs that can be detected in turned components [11]. A common method to highlight the presence of these unwanted elements is visual inspection performed by trained operators in quality laboratory. Visual inspection is performed using image magnification systems and rotating the sample so that the operator can identify the presence of eventual burrs either in the inner or the outer surface of the sample under test (Fig. 4.1 right).If burrs are detected the sample is reworked, thus increasing production time and cost. Being a manual control, this inspection cannot be performed on a 100% basis, therefore the risk of missing samples not compliant for the presence of burrs is high.

Machine vision plays a very relevant and increasing role for in-line quality control, because vision systems can be designed to mimic a variety of visual inspections normally done by expert operators. Vision systems for in-line quality control span over a wide range of complexity, from a single fixed camera and steady illumination[22], to moving cameras on robot arms in eye-in-hand configuration

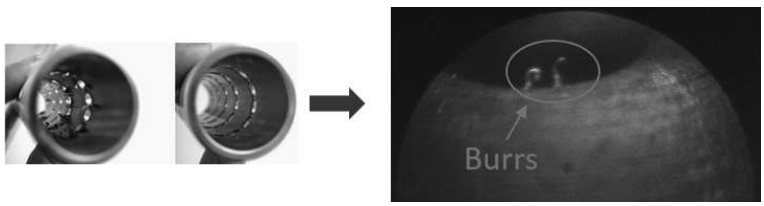

Figure 4.1: Quality control system for burrs identification: Typical visual inspection of burrs performed manually by an operator.

[50], with adaptive illumination [65], or structured illumination [17], just to mention a few solutions that can be found in manufacturing lines. Bearing in mind this thought, when considering a quality control system based on vision for in-line inspections, the first and most important step is the design of the system lay-out, including illumination, imaging optics, camera and image acquisition. In real industrial applications of vision in production lines, which are noisy, sometimes dirty, environments, with variable lightning conditions, variable optical characteristics of target surfaces, this is of the utmost importance for the achievement of the final result. The algorithmic part is as important, but it is necessarily the second step to be addressed. In the following paragraphs an automatic system for burr inspection, based on a machine vision, is presented.
This solution has been patented to protect the idea developed [54]. The application was filed jointly by Università Politecnica delle Marche and Zannini SPA. I was one of the inventors among the UNIVPM team. At the time of the patent filing the ownership was 50% each. Zannini SPA, then, acquired the UNIVPM share, thus realizing a complete technology transfer, which will hopefully trigger the industrial exploitation of the idea developed within this thesis.

4.2 Design and realization of the quality control system: Hardware

An optical arrangement with a camera observing the sample from outside in back-light condition (sample between camera and illuminator) was developed. This set-up makes it possible to detect burrs as modifications of a circular shape; this requires the use of telecentric lenses [7] to eliminate distortions due to perspective.
A light stick diffusive illuminator, to be placed inside the sample, has been specifically developed for the purpose, because there are no commercially available solutions that are simultaneously able to provide a 360° illumination condition and be inserted in bores of 11mm maximum diameter. Different materials and surface finishing conditions of the light stick have been tested, as well as the possibility of exploiting RGB LED to change light colour depending on the environmental illumination. This smart feature will be described in detail in the following section.

4.2.1 Lay-out and Hardware architecture

The main idea of the system is to imitate, in an automated way, the inspection performed by an operator. Indeed, the part is generally checked by an operator who rotates it and observes the shape of each hole from the outside. In the same way, the operator can be substituted by an machine vision system that inspect each hole from the outside in back-light configuration while the part is rotated. Backlighting is provided by a custom light stick inserted inside the piece under examination(Figure 4.2).

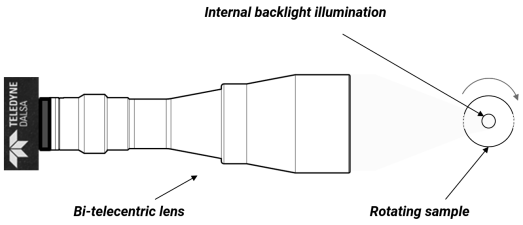

Figure 4.2: Quality control system for burrs identification: Operating principle of the system to detect burrs.

The basic layout of the system is shown in Figure 4.3. The fingers of a robot gripper make it possible part to be grasped, centered and rotated. Two cylindrical illuminators are inserted axially inside the hollow cylinder under control to observe it in backlight condition. The backlight image of the side holes of the piece is acquired with a camera and telecentric optical system oriented orthogonally to the cylinder axis under inspection. Below is the description of each component.

4.2.2 The backlight diffuse illuminator

To observe each hole in backlight is necessary that a backlight illuminator is operating from the inside of the part.
The illuminator I developed is a transparent polymeric cylinder with a rough surface; light is fed to the light stick by a LED source connected on its base and travels along the cylinder. Due to light source divergence and to light scattering within the core of the polymeric cylinder, light reaches the rough surface of the cylinder which acts as a diffuser. Hence light is diffused radially and, once the illuminator is inserted inside the hollow cylinder to be inspected, its inner surface is illuminated over the full length over the 360°, below how the illuminator is made.

As a light guide, the internal light stick illuminator aims to transport light from a light source (e.g. a LED source) to a point at certain distance with minimal loss. Generally the light is transmitted inside a light guide through total internal reflection. To explain this concept it is necessary to start from the Snell's Law (4.1): a beam of light incident to the boundary between

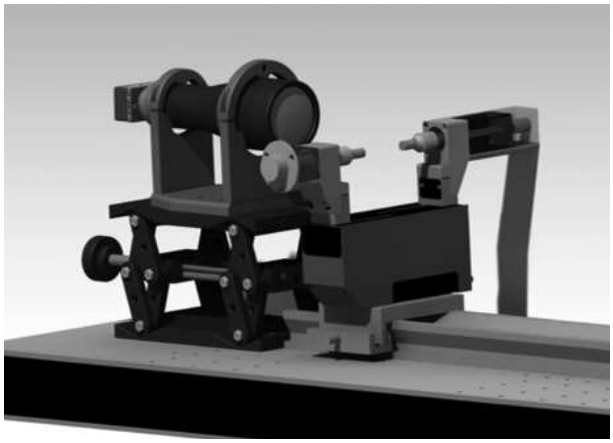

Figure 4.3: Quality control system for burrs identification: Lay-out of the system. Clearly visible: camera, telecentric lens, gripper with backlit internal illuminator and rotating actuator.

two different mediums, i.e. plastic and air, is refracted when it crosses the border as shown in Figure 4.4.

$$n_i sin\phi_i = n_f sin\phi_f \tag{4.1}$$

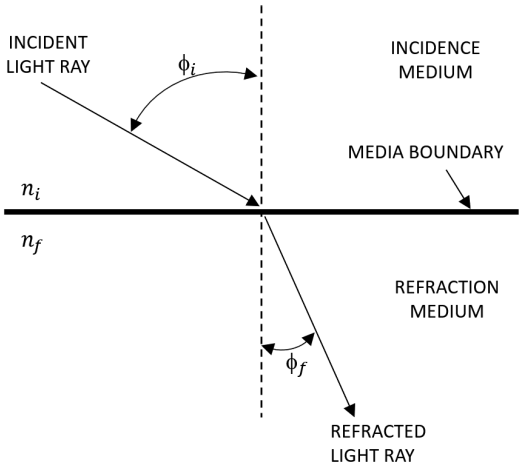

Figure 4.4: Quality control system for burrs identification: Refracted Light Ray.

Where ϕ_i, called angle of incidence, is the angle at which the light beam si incident to the boundary and the angle at which the light rays leave the boundary is called the angle of refraction, ϕ_f. Snell's law states: the index of refraction of the first medium, n_i, multiplied by the sine of the angle of incidence at the boundary, ϕ_i, is equal to the index of refraction of the second medium, n_f, multiplied by the sine of the angle of refraction at the boundary, ϕ_f.

If the angle of incidence increases to the point where the angle of refraction is 90° the incident light ray is refracted along the boundary, as shown in Figure 4.5. The $\sin\phi_f\ (90°) = 1.0$, and Equation 4.1 for Snell's law reduces to: $n_i \sin\phi_i = n_f$. This expression can be rewritten to define the critical incident angle for total internal reflection, ϕ_c (called critical angle, 4.2):

$$\sin f_c = \frac{n_f}{n_i} \tag{4.2}$$

By knowing the air's index of refraction and bringing it into the equation 4.2, $n_f = 1.0$, it is possible to calculate the critical angle. For most plastics and glass, the index of refraction is

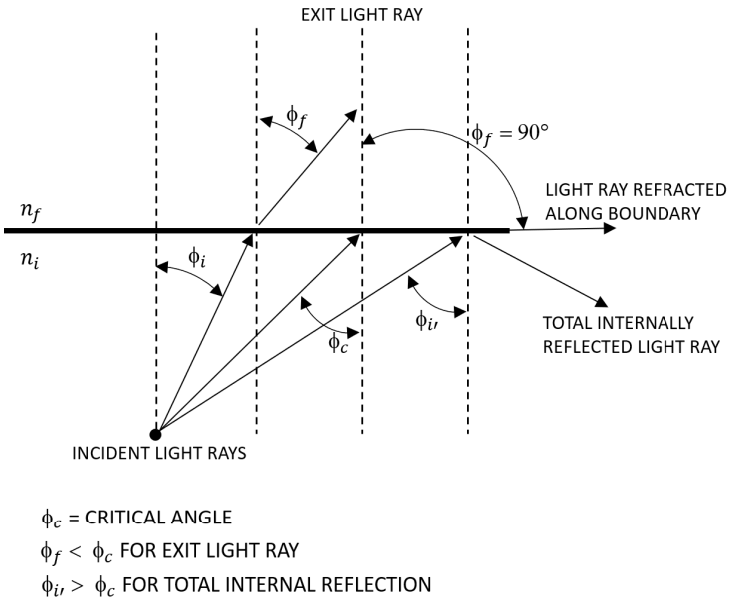

Figure 4.5: Quality control system for burrs identification: Definition of critical angle for total internal reflection.

approximately 1.50 and the critical angle for the total internal reflection is approximately 42 °. Therefore for angles greater than the critical angle the light beam is totally internally reflected.

In case of light guide it is not just about total internal reflection as when a light beam crosses the boundary through one medium to another there is a loss due to the reflection on the surface which is represented in Figure 4.6. This is called Fresnel loss, is defined when the angle of incidence equals the angle of reflection and is calculated with the following expression 4.3 :

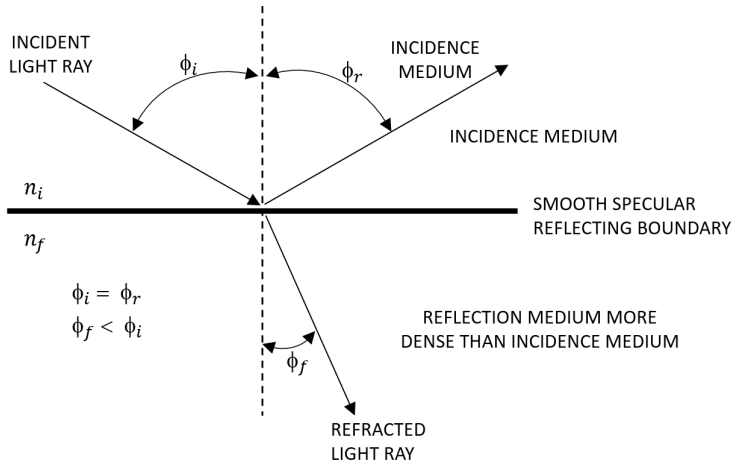

Figure 4.6: Quality control system for burrs identification: Specular reflected light ray at mirror smooth boundary (Fresnel loss).

$$Fresnel\ Loss = 100 \cdot \left[\frac{n_i - n_f}{n_i + n_f}\right]^2 \tag{4.3}$$

For plastic to air and glass to air interface boundaries, the Fresnel loss is approximately 4 %. During the design of a light guide, there are two main aspects to consider:

- Coupling between LED and light guide with minimal loss;
- Allowing light to escape through the exit surface with minimal loss.

About the design of coupling between LED lamps and the entrance of light guide, flux coupling and capture are usually ineffective when the light is placed externally to the light guide. If the LED lamp is external to the light guide (Figure 4.7), most of the flux will be lost (10% of the available flux is captured with this configuration).

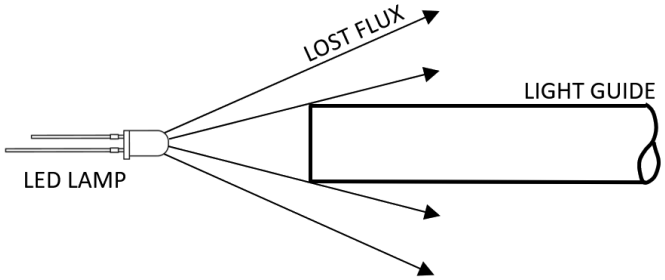

Figure 4.7: Quality control system for burrs identification: LED Lamp External to Light Guide.

With a lens it is possible to focus the flux when the LED light is external to the light guide (Figure 4.8) increasing the captured light up to 80%.

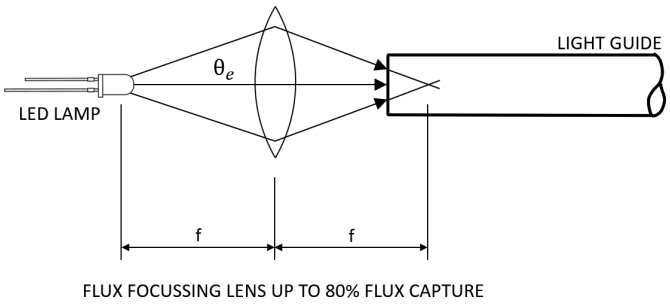

Figure 4.8: Quality control system for burrs identification: Using a Lens to Focus LED Light Onto Light Guide.

However the best coupling configuration is to have the LED light located inside the light guide as shown in Figure 4.9.

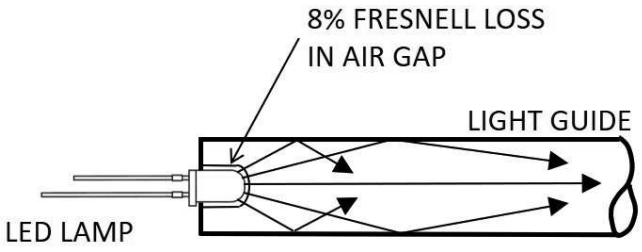

Figure 4.9: Quality control system for burrs identification: LED Lamp Located Inside a Light Guide for Best Flux Coupling.

The light captured will be between 92% and 100%, taking into account the Fresnel losses across the air gap between LED light and light guide (Figure 4.10).
The maximum percentage of this configuration is reachable by:

- Glowing the LED light to the light guide;
- Using index matching fluid;
- Realising a perfect coupling between both elements in order to not having an air gap.

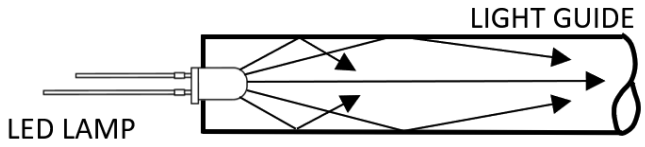

Figure 4.10: Quality control system for burrs identification: LED Lamp index matched inside a Light Guide to Eliminate Fresnel Loss

As a physical attribute of a Light Guide, the exterior surface finishes are important to assure proper operation.
The sides parallel to the direction of light travel should be smooth to works in total internal reflection. The entry surface must be smooth, shaped to adapt to the LED lamp device for effective light insertion, allowing light rays to enter the light guide with minimal reflection and dispersion. The exit end should be diffused. A diffused exit end has random critical angles across its surface providing a high probability light rays can escape, and also scatters the light rays producing a wide radiation pattern.

In my case the illuminator is an object that works halfway between a diffuser and a light guide. The LED lamp is coupled to one of the base surfaces of an acrylic rod cylinder. Anyway the light must come out of the lateral surfaces of this stick cylinder; for this reason the lateral surfaces must be rough.
A diffused lateral exit end (rough surface) presents random critical angles to internal light rays, assuring the probability of light escaping from the illuminator. This may also be viewed as the diffused exit end having random indices of refraction. The exiting light rays are disbursed at random angles into a wide radiation pattern of light, as shown in Figure 4.11.

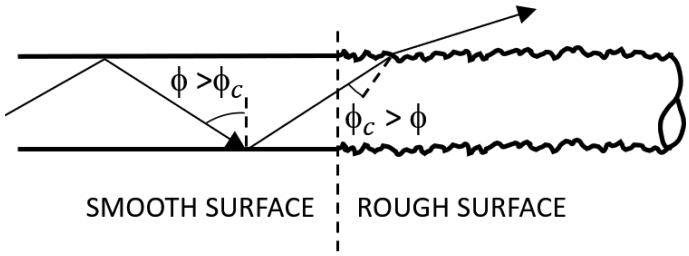

Figure 4.11: Quality control system for burrs identification: Lateral Diffused Exit End Enhances the Probability of Light Escaping the illuminator.

An illuminator made as in Figure 4.12, has problems related to the diffusion of light. the intensity of light coming out of this type of illuminator is greater near the LED lamp and decreases as the length of the illuminator increases.

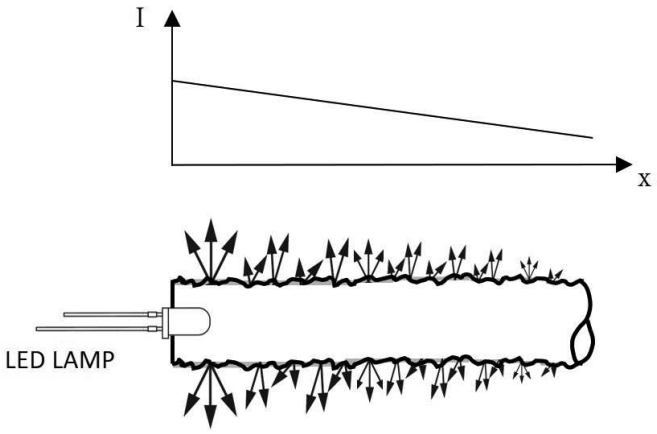

Figure 4.12: Quality control system for burrs identification: Decrease in intensity of light in diffusive cylindrical illuminator.

To make the inspection of the burrs automatic, I chose to use two identical illuminators which, during the gripping of the piece, are inserted inside it until they merge with each other. This choice helps both in the mechanical aspect during the gripping phase, both from the optical point of view thus ensuring higher illumination efficiency and uniformity along the illuminator length. In fact, observing the intensity of light coming out of a single illuminator, it tends to decrease as it moves away from the LED source; shaping the terminal surface of the illuminator in a very smooth way (Figure 4.13), the light passes from one illuminator to another, strongly reducing the intensity gradient light between the extreme points of each illuminator (Figure 4.14).

Figure 4.13: Quality control system for burrs identification: Smooth end exit coupled with the second illuminator to transmit light.

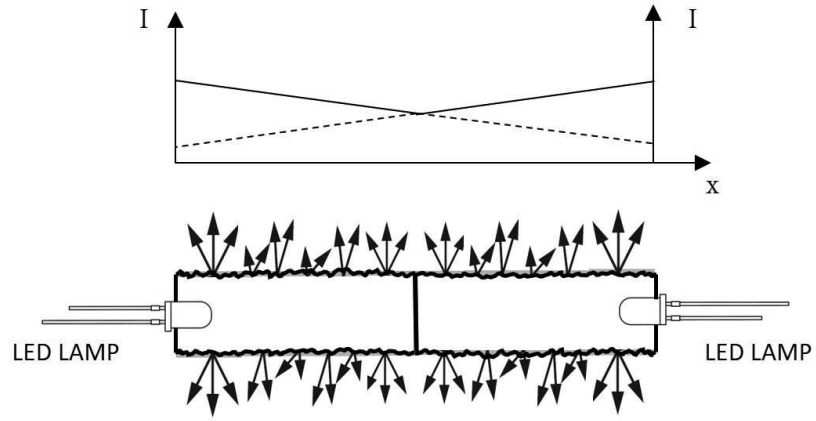

Figure 4.14: Quality control system for burrs identification: two coupled illuminators to reduce the decay of light intensity.

The first pair of illumnators designed and created were 3D printed (Fig. 4.15) using a stereolithography (SLA) printer in transparent resin then solidified. Through 3D printing it is possible to realize the perfect coupling between the illuminator and the LED source with Concave Entrance End that increases Flux coupling Figure 4.16. The lateral surface of the illuminator was made rough by sandblasting.

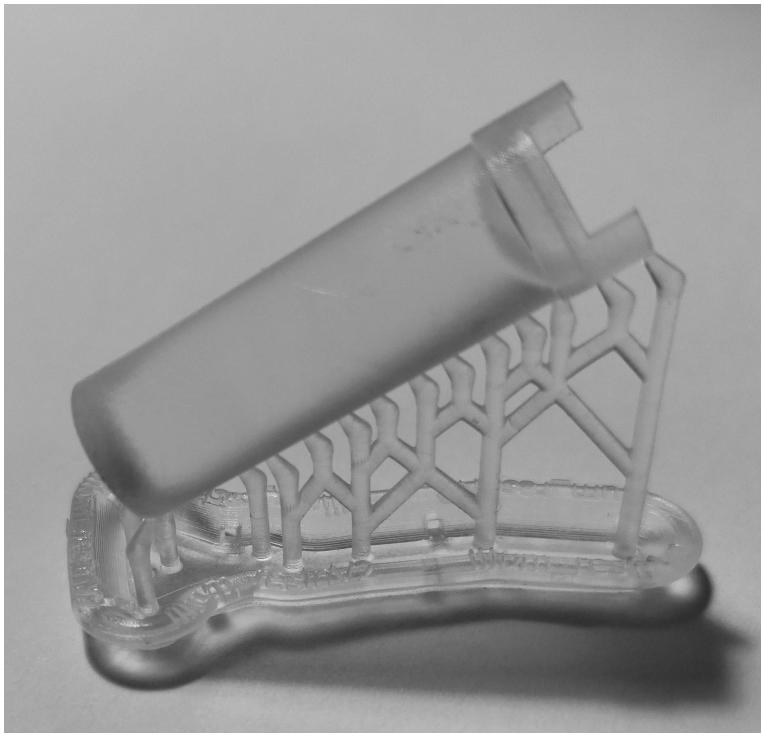

Figure 4.15: Quality control system for burrs identification: 3D printed illuminator.

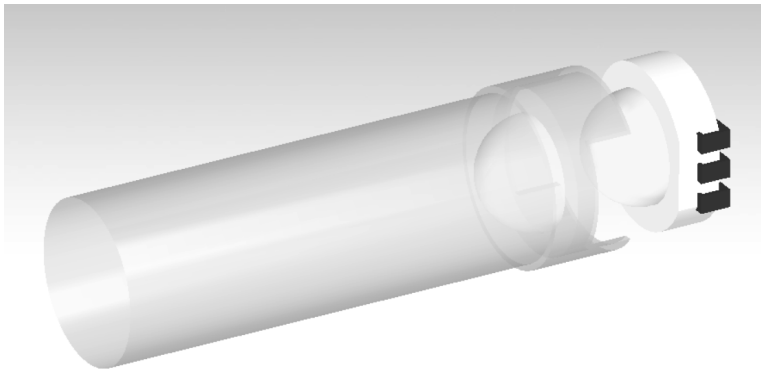

Figure 4.16: Quality control system for burrs identification: Illuminator with concave Entrance End that improves Flux Coupling.

Although presenting a concave entrance, as suggested in [67] with this configuration about 70% of the available emitted flux from an LED is captured by the light guide, and the light loss is reduced to 20% to 30%, at the moment of coupling between the two illuminators, that is when the two fingers close, the clamping force also affects the hemispherical lens of the LED. The LED was damaged after few piece loading-unloading cycles, thus reducing the robustness of the inspection system.
The need to have a rugged system to implement in a real industrial scenario forced me to design a second version of this illuminator.

The final version of my illuminator consists of two cylinders 25 mm in length obtained from a plexiglass rod with a diameter of 8 mm. These cylinders are first sandblasted so as to have a lateral surface which allows light to exit; the base surfaces of the cylinder are honed so as to guarantee the best coupling light flux with lower losses.
As shown in the Figure 4.17 the two illuminators are coupled together on one of the two base surfaces and the led on the other.

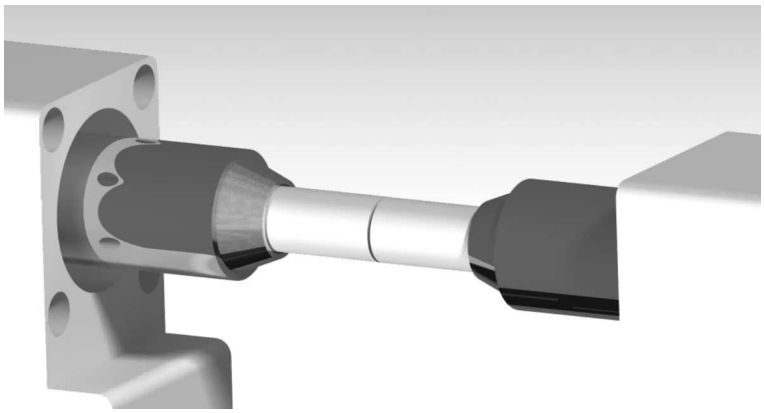

Figure 4.17: Quality control system for burrs identification: Coupling of the two illuminators.

More in detail, the LED is inserted inside an hollow cylinder (Figure 4.18) that contains it and into which transparent epoxy transparent resin is cast.

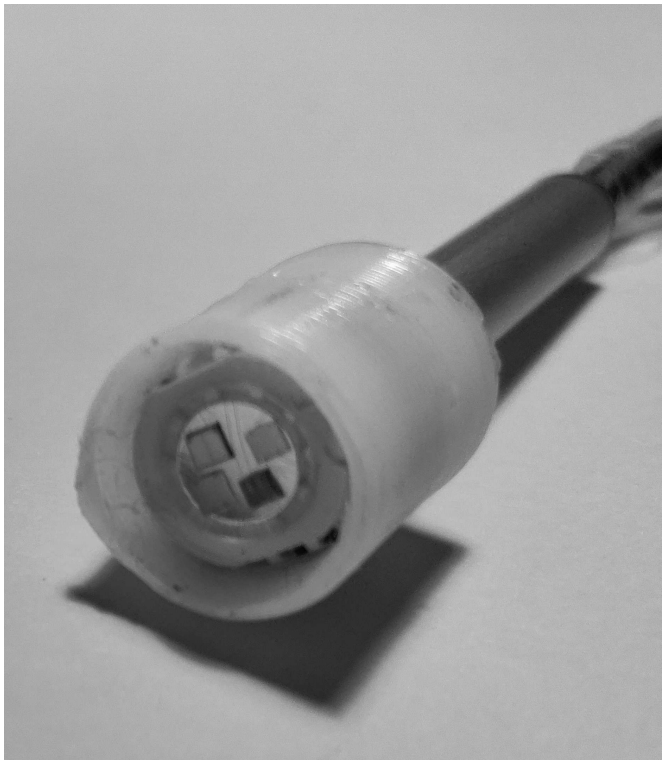

Figure 4.18: Quality control system for burrs identification: Hollow cylinder that contains LED.

Once the resin has dried, it is honed. From this surface direct light exits the illuminator and the coupling flux is be guaranteed by the gripper's clamping force (Figure 4.19).

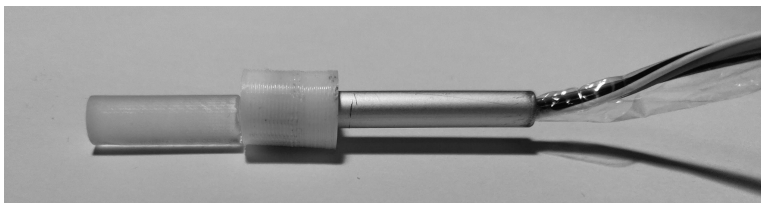

Figure 4.19: Quality control system for burrs identification: cylindrical illuminator coupled to a resin coated LED.

The LED light source is 3 Watts RGBW (red, green, blue and white) LED with eight leg (four anode and four cathode)(Figure 4.1). The technical specifications are shown in table 4.20.
This feature enables image optimization (contrast enhancement) with respect to environmental light and the optical characteristics of the part.
The hemispherical lens on the top of the LED guarantees a light beam angle of 140° which coupled with the illuminator makes it possible to spread light laterally, This allows an external observer to see the light exiting from the lateral holes; burrs will appear as black shades over a luminous circle.

Table 4.1: Quality control system for burrs identification: Technical data of the RGBW LED.

	Wavelength, Colour Temperature	Luminous Flux
Red	620-625 $[nm]$	70-80$[lm]$
Green	520-525 $[nm]$	130-150$[lm]$
Blue	460-470 $[nm]$	30-40$[lm]$
White	6000-6500$[K]$	110-120$[lm]$

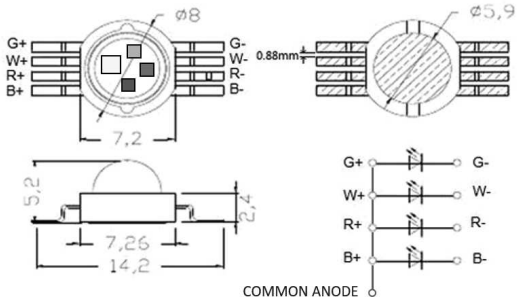

Figure 4.20: Quality control system for burrs identification: Led RGB+W.

The LED colours and intensity are managed by a microcontroller through a power driver (Figure 4.21).
The driver chosen is particularly suitable for the management of LEDs of this type, offering the possibility of being powered by 6 ÷ 36 Vcc, The driver also guarantees a maximum output current of 1 A per channel and has four output channels, in this way the four colours of the LED can be managed individually in a separate way.
Table 4.2 shows the technical specifications of the driver.

Table 4.2: Quality control system for burrs identification: Technical data of the LED driver.

Supply voltage	6 ÷ 36 Vcc
Maximum current output	1 A per channel
Dimming	Analogical and digital
Number of channels	4
Dimensions	27,6 x 37,3 mm

The LED can be controlled in the following way:

- When a DC voltage lower than 0.4 volts is applied to the CTRL pin, the converter turns off and the output goes to zero volts;

- Applying a PWM signal on the CONTROL pin, the output is set according to the duty-cycle of the signal itself, with a resolution of 1,024 steps.

As already explained Two RGBW led must be controlled both to combine more colours simultaneously and to change the intensity of light with respect to environmental light and the optical characteristics of the part (Figure 4.22).

The two illuminators can rotate together with the piece and the cone, therefore it was necessary to insert two slip rings for powering the LEDs also during the rotation.
Since the LED wires must be place inside the drive shaft and the driven one (as will be shown in the next paragraph), and since each slip ring has at most 6 possible connections, I chose to connect all the LEDs anodes together.

In this way 5 connection wire per LED are used: a common positive pole and four negative ones each to control a different colour.
Figure 4.23 shows the wiring diagram for the control of LEDs with power drivers and microcontroller.

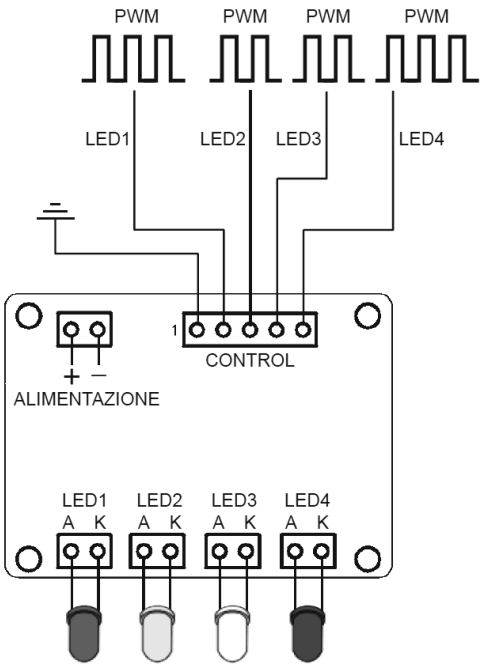

Figure 4.21: Quality control system for burrs identification: Connection diagram of the driver and control via PWM signals.

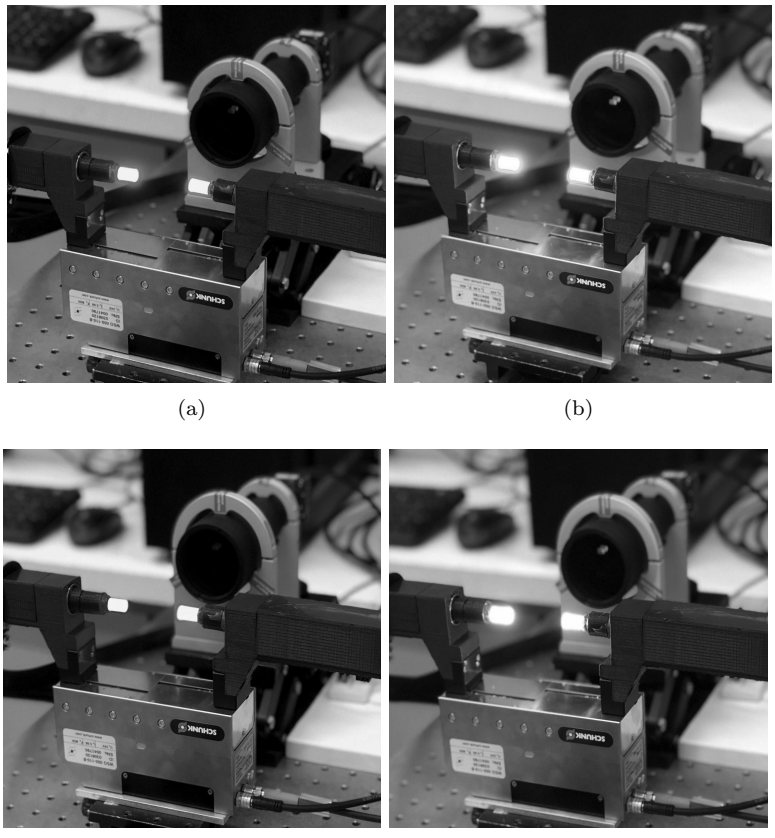

(a) (b)

(c) (d)

Figure 4.22: Quality control system for burrs identification: Colour control of the RGBW LED

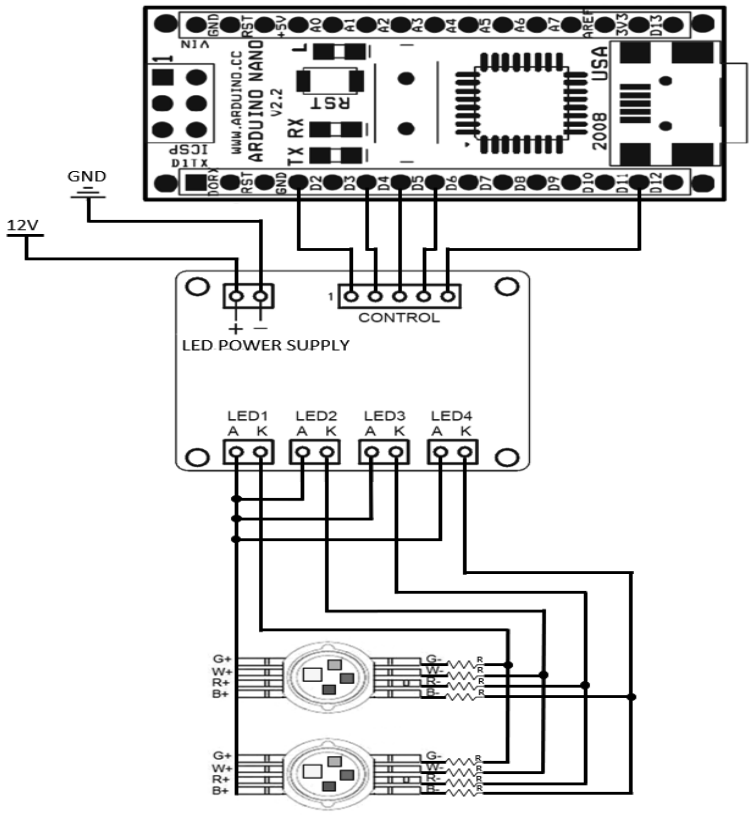

Figure 4.23: Quality control system for burrs identification: Electric scheme of the Led RGB+W controlling units.

4.2.3 The gripper

In order to automate the system, the diffuse internal illuminator is realized in two parts, which can be inserted from the two opposite sides of the hollow cylinder. Each part is mounted on one finger of a robot gripper which allows insertion of the illuminator inside the hollow cylinder. Two conic elements allow centering the hollow cylinder with respect to the internal diffuse illuminator. The conic elements can rotate axially, under the action of a stepper motor mounted on one of the fingers. Once the fingers are closed, and the conic parts block the hollow cylinder, the stepper motor can rotate it. This allows a fixed camera to observe in sequence all the outer surface of the cylinder; lateral holes will appear as luminous circles over a black surface, thanks to the inner backlit diffuse illuminator.
Loading and unloading of the hollow cylinder onto the gripper is done by a robot arm; however, the system can also be operated by a human operator.
The whole system configuration is shown in Figure 4.24, in both open and closed configurations.

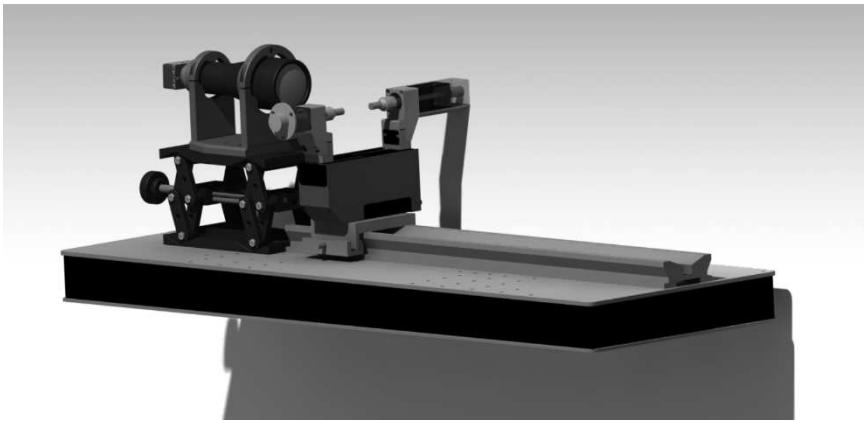

(a)

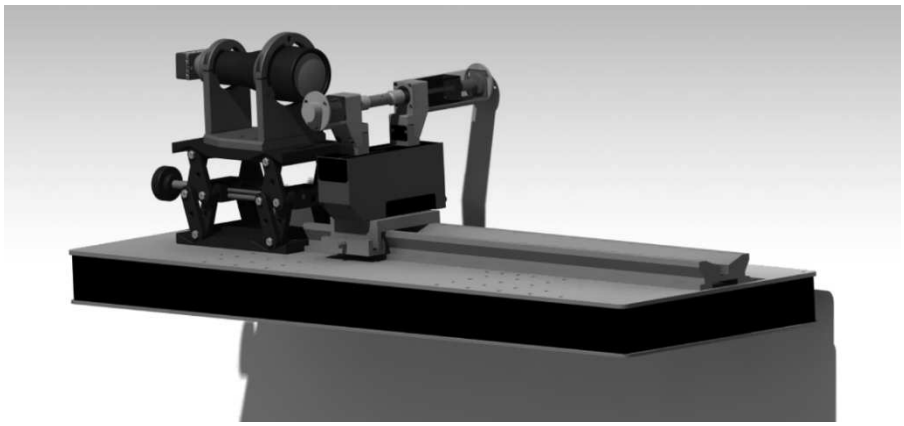

(b)

Figure 4.24: System for detecting burrs

I chose to use the Network-enabled Schunk WSG 50 Gripper that combines a long stroke and precise (encoder feedback) movement. Speed and gripping force are controlled. The technical specifications of the gripper are shown in table 4.3.

Table 4.3: Quality control system for burrs identification: Technical data of the gripper WSG 050-110-B.

Min. gripping force $[N]$	5
Max. gripping force $[N]$	80
Recommended workpiece weight $[kg]$	0.4
Max. permissible finger length $[mm]$	170
Max. permissible mass per finger $[kg]$	0.3
Repeat accuracy $[mm]$	$\pm$ 0.03
Max. speed $[mm/s]$	420
Max. acceleration $[mm/s^2]$	5000
Communication interface	EtherNet TCP/IP, PROFIBUS, CAN

Figure 4.25 shows the section of the custom gripper. The stepper motor is mounted on the black finger; the shaft is connected to the slip ring at the back. The slip ring allows to power the LED during its rotation. The wires from the slip ring pass inside the hollow shaft to the top of it. In the front part of the shaft, there are the centering cone, led and illumination system.
Two ball bearings, which ease the rotation of the shaft thy hold, are mounted on the green finger. Also this shaft is connected in the rear part to a slip ring for powering the LED.The cone, the LED and the illumination system are keyed to the front.
It is necessary to guarantee friction between the two cones and the part under inspection so as to

allow their integral rotation. Moreover, it is necessary that the top parts of the two illuminators are coupled to make light intensity uniform, as described in Figure 4.14.
I developed a system contained within the cone (Fig. 4.25) connected to the motor shaft, which, through a coil spring, pushes an illuminator towards the other; at the same time, however, it ensures that all elements connected to each other (cones and piece) rotate without slipping.
when the piece is tightened between the two cones, the illuminator not connected to the motor pushes against the other which can move backwards keeping their connection (thanks to the coil spring) for the light transfer.

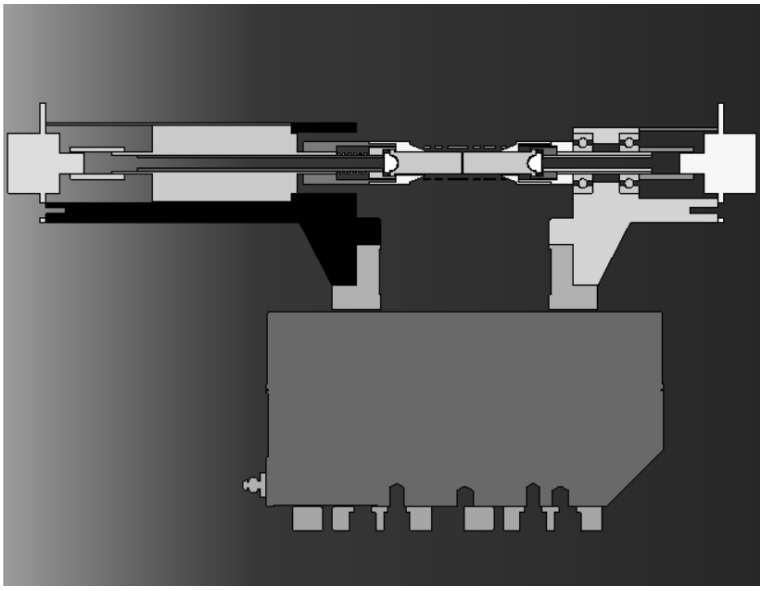

(a)

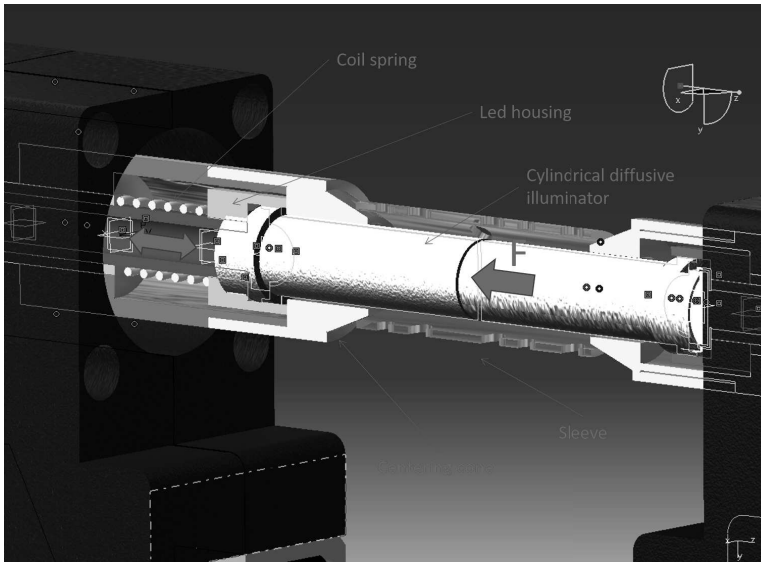

(b)

Figure 4.25: Quality control system for burrs identification: Custom gripper in section: whole 2-D gripper section (a) and 3-D close-up of the retractile illumination system.

As for the control of the LEDs a dedicated driver connected to the micro-controller is needed to manage the motor. The electric scheme of the motor management devices is reported in Figure 4.26: the stepper motor is controlled by a PWM signal generated by the microcontroller and sent to the power driver, which takes care of transferring it to the motor.

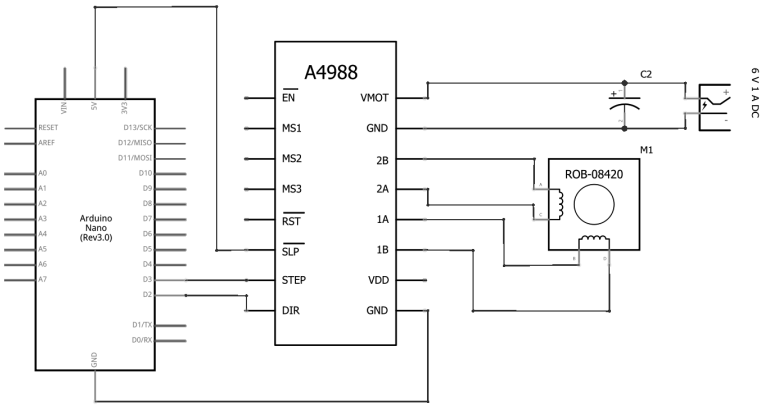

Figure 4.26: Quality control system for burrs identification: Electric scheme of the motor controlling units.

4.2.4 The camera and lens

The hollow cylinder under inspection is positioned orthogonally to the optical axis of the objective and with its own axis horizontal (see Fig. 4.24). A bi-telecentric lens, with field of view of 34.98 mm × 29.18 mm, was selected for the inspection; this guarantees correct framing whose dimension is lower than 30 mm over a depth of field of 11 mm. The contrast transfer function (CTF @ 70 lp/mm) is larger than 40%, thus assuring an optical spatial resolution better than a_{opt} <0,014 mm. We have a CMOS camera (Fig. 4.27)having a 2/3“ chip, with 2464 × 2056 pixels was selected for being coupled to the lens. The camera is operated in ROI mode; this was done with the purpose to reduce the image size and speed up the frame rate (current frame rate: 200 fps). Overall, the system allows for a spatial resolution of less than a_{sens} <0.015 mm (no sub-pixeling considered). Camera resolution combined to optical resolution limits the detectable burr size to a <0.02 mm: however, burrs are expected to always exceed this dimension.

Figure 4.27: Quality control system for burrs identification: Matrix vision CMOS camera.

The camera is not triggered for the acquisition. This choice was adopted because the small hardware ROI investigated made it possible to increase the image acquisition frame rate, thus working in ”oversampling” condition. This redundancy of data makes the presence of a trigger irrelevant.
The table 4.4 shows the technical specifications of the camera

Table 4.4: Quality control system for burrs identification: Technical data of the camera RT-mvBF3-2051G.

Sensor size	2/3”
Resolution [$pixel$]	2464 x 2056
Pixel size [μm]	3.45
Frame rate [Hz]	80.5
Shutter type	Global Shutter
Sensor name	Sony IMX250
Sensor type	CMOS monochrome
Interface	USB 3.0 (5GB/s)
RAM	256 Mb

4.3 Design and realization of the quality control system: Software

The images are acquired and processed in the pre-defined Region of Interest identified by the green rectangle in Figure 4.28.

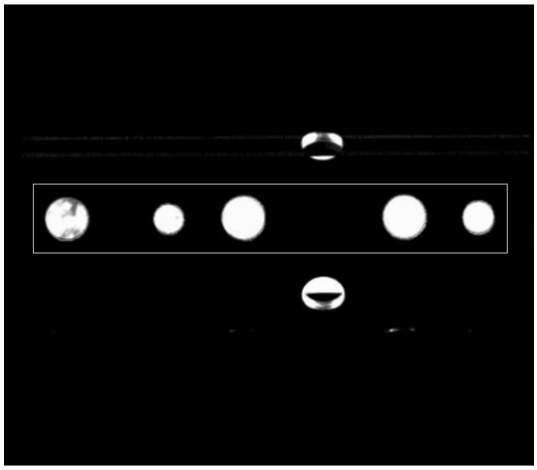

Figure 4.28: Quality control system for burrs identification: Burrs detection Region of interest.

Figure 4.29 reports a typical image acquired on holes which are close to orthogonal to the optical axis of the telecentric vision system within the ROI. On the right a zoom allows to see a burr highlighted by a red circle.

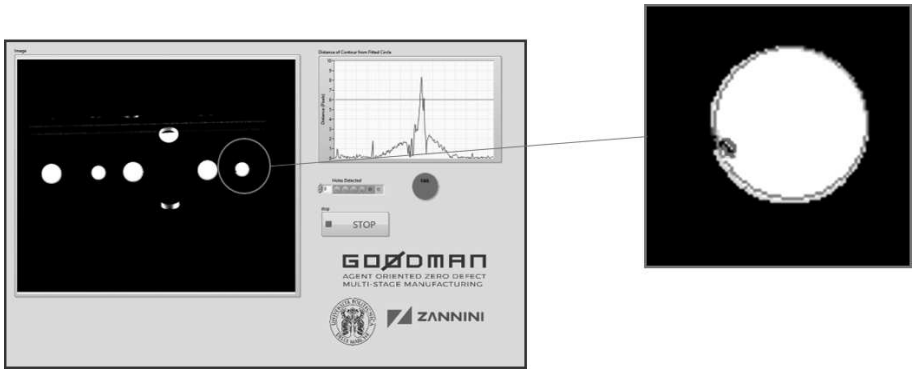

Figure 4.29: Quality control system for burrs identification: Typical image and zoom on a hole with a burr.

Burrs recognition is based on a geometric pattern matching algorithm [33]. Indeed, this algorithm is exploited to highlight dissimilarity with respect to known geometric shapes [73]. With respect to standard pattern matching approaches, in which pixel intensity levels in the template image are used for matching on the final image, the algorithm exploits geometric information present in the template image as primary features (e.g. low-level features, like edges or curves, or higher-level features, such as the geometric shapes made by the curves in the image) for matching. Deviations from known geometric features are then compared to a threshold: if some data falls above the threshold, these data, very likely, correspond to burrs on the hole.
More in detail, as reported in Figure 4.30, after acquiring an image, the search for circles is carried out. on the identified circles, an annular ROI is applied. From each applied ROI, the hole contour is extracted and the best fit circle of the hole is identified; The calculated distance between contour and best fitted circle is compared to a threshold. If the distance is less than the threshold, no burrs are present.
The final result related to the control of the part is given by a logical OR performed with the

results of the single distance comparisons. This choice is based on the need to discard the pieces with burrs, even in the presence of only one burr (from which the reason of the logical OR).

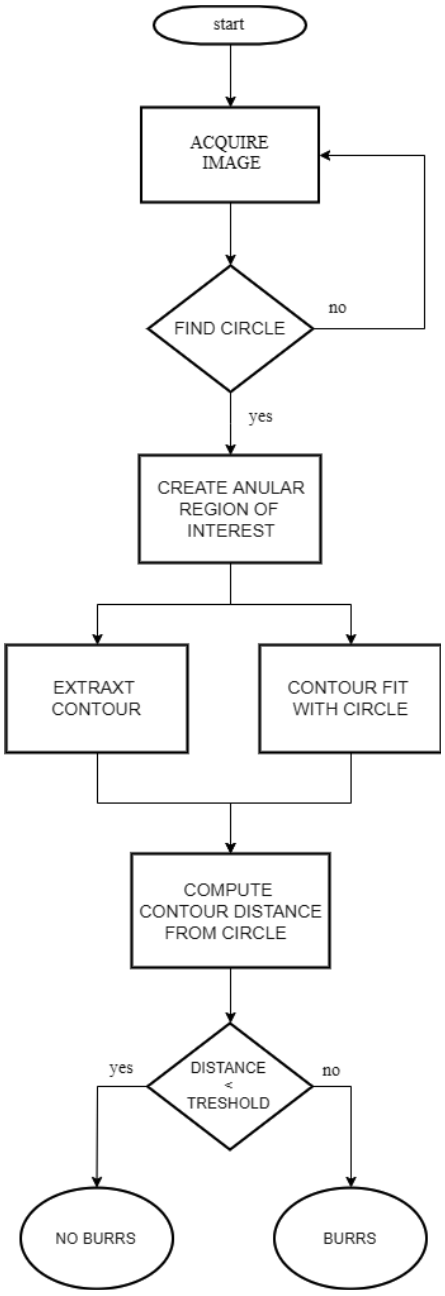

Figure 4.30: Quality control system for burrs identification: Burrs detection machine vision algorithm.

The measurement sequence follows the procedure reported in the flow diagram of Figure 4.31). The system waits for an external trigger event; in the automatic version, it will be a hardware trigger provided by the robot (and exchanged using TCP-IP communication protocol) placing the hollow cylinder onto the gripper; in the manual operating mode, the part is charged onto the gripping system by the operator, and trigger is provided via a push button on the system's HMI (Human Machine Interface). Once this trigger has been received, the part is then closed by the gripping system and the internal illuminator inserted accordingly. The colour of the illuminator light is adjusted depending on environmental light and/or the part finishing; this is a smart behaviour which aims to keep image contrast as high as possible. After this adjustment the part is

brought to rotation and the measurement starts. If data are not consistent to predefined confidence level after one rotation (e.g. clockwise), rotation direction is inverted (e.g. counter clockwise) and inspection is performed again.

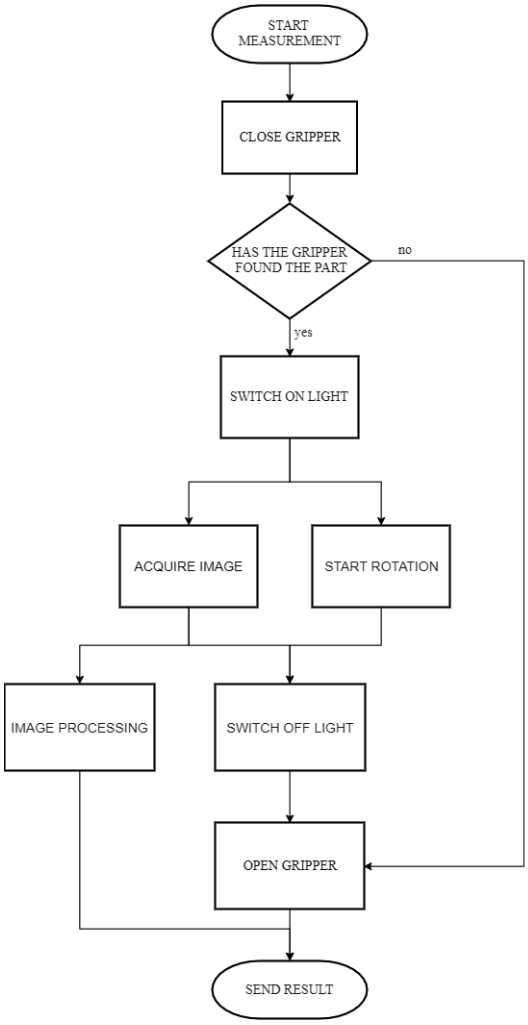

Figure 4.31: Quality control system for burrs identification: Burrs detection measurement procedure.

4.4 Results in a real production line

A validation testing campaign, which aimed to ensure equal/superior performance of the system to the inspection strategy currently used in ZANNINI, has been performed in ZANNINI Poland' facility. A batch of 2000 parts was tested using manual charge/discharge onto the burrs inspection system. Inspection was performed on 100% of the batch and double-checked by the standard burrs inspection approach adopted by ZANNINI Poland's quality operators. Before the validation phase, the threshold to be used in the algorithm was identified running dedicated tests on a batch of healthy parts (batch of 100 parts).
The validation test identified no damaged parts among the batch produced. Actually, 5/2000 false positives came out after an initial screening. However, it turned out that these false positives were due to a wrong charging of parts onto the gripping system. Consequently, a further test of these 5/2000 parts with the burrs inspection system revealed their healthy nature.
The system has been exploited in a bigger demonstration phase (overall batch production: 20000 parts) running in ZANNINI Poland within the GO0D MAN project from June to September 2019. The inspection can take place either in automated mode (part placed on the system by a robot) or it can be run by a human operator (current installation – Figure). A dedicated HMI shows the inspection result as well as the percentage of scraps identified over the total parts inspected. Data recorded by the system are stored locally on a local database and sent to the MAS system.

(a) (b)

Figure 4.32: Quality control system for burrs identification: automated (a) vs manual (b) set-up

The inspection system provides an overall information related to the presence of burrs on the part. Consequently, the result is binary (Good/Scrap) and no acceptability ranges have to be considered. No particular issues should be reported for the GO0D MAN production lot.

Data reported hereafter refer to the monitoring period 28/06/2019 – 28/08/2019. The dataset consists of 23545 parts. Figure 4.33 reports the distribution of scraps vs good parts.

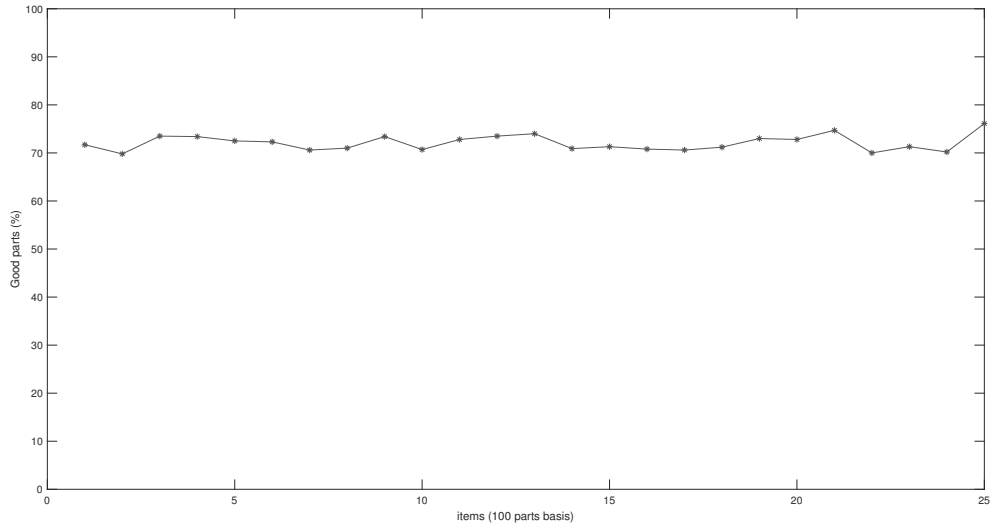

Figure 4.34: Quality control system for burrs identification: Evolution of results for the monitoring period 28/06/2019 - 28/08/2019. Data are down sampled to get 1 sample = percentage of good parts over a basis of 100 parts.

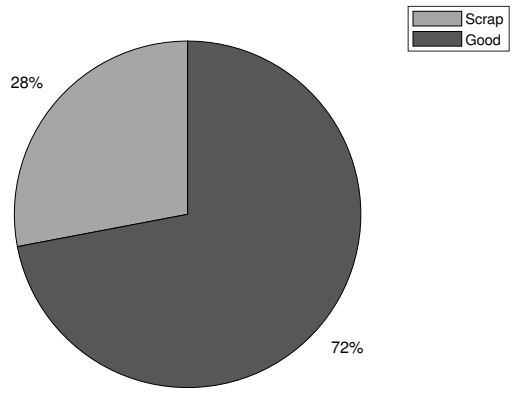

Figure 4.33: Quality control system for burrs identification: Scrap analysis for the monitoring period 28/06/2019 - 28/08/2019.

To check the stability of the process and the quality control station results of bit have been down sampled (1 sample = good parts over a basis of 100 parts) and tracked in their time evolution. As it can be seen from Figure 4.34, the combination of process and performance of bit (it is not possible to separate them) is stable over the whole dataset.

Chapter 5

Conclusions

This thesis is focused on the development of two Quality Control Systems for in-line inspection of 100% of production.
This research is part of the European Project GO0D MAN-"aGent Oriented Zero Defect Multi-Stage Manufacturing". GO0D MAN project has received funding from the European Commission under the EU Framework Programme for Research and Innovation Horizon 2020 (2014 - 2020) within the FoF – Technologies for Factories of the Future initiative. Contract no. H2020-FOF-03-2016-723764.
In particular, the European project deals with identifying the path to zero-defect production by integrating and combining process and quality control for multi-stage manufacturing into a distributed system architecture built on agent-based Cyber-Physical Systems and smart QCS.
The presented work has been carried out on the Zannini use case targeting the development of two different QCSs for assessing the geometric and functional tolerances (absence of burrs) on high precision turned sleeves for automotive hydraulic electro valves, i.e.:

- A quality control system to automatically measure internal diameter and length in cylindrical parts by contactless technology;
- An automated inspection system to detect the presence of burrs.

The first of the two systems developed has the purpose of measuring geometric features inside these sleeves. The latter are characterized by a very small internal diameter and internal grooves. The inline statistical quality control solution adopted before GO0D MAN involves human operators who use manual gauges for internal diameter measurement and caliper for length measurement. These instruments, although precise, have some drawbacks, e.g.:

- Must be manually managed by the operator;
- They need dedicated gauges compliant to the different diameters produced;
- Cannot measure on inner grooves.

Moreover, only Statistical Process Control can be adopted, because monitoring of 100% of production would necessitate too much time, given the high production rate.
An automatic station to measure the internal diameter and length of these sleeves was therefore developed. The station exploits a confocal chromatic sensor that makes it possible to measure without contact both the part internal diameter and its length. In fact, the probe diameter is compatible with the internal diameter of the sleeves. The selected sensor has a 90° beam exit which allows to measure the radius of the sleeve. This type of sensor is usually used in relative distance measurements or to measure the thickness of transparent objects, hence dedicated solutions were adopted to measure direct distances and compensate the influence of temperature variations which can happen in a production line.
The station has 4 degrees of freedom; micrometric stages allow the sensor to be inserted inside the piece to be inspected, rotate and scan a certain section of the part. The micrometric stages under the part allow to centre its axis with respect to the sensor, reducing the fluctuation of the datum

with respect to the nominal value. Since the GRIN lens inside the sensor is sensitive to temperature variations (refractive index temperature dependent), a dedicated procedure to compensate for temperature fluctuations have been developed. Dedicated tests in laboratory conditions were run to optimize the testing set-up and measurement procedure, as well as to estimate the measurement uncertainty characterizing the QCS. The system has worked in a real production line (Zannini Poland) at the outlet of a turning machine for three months 24/7. Although the use of the developed measuring station was limited to the measurement of turned components for automotive use, this can be extended to all the applications for which it is necessary to carry out measurements inside small cavities.

The second quality control system developed is related to the inspection of the presence of processing burrs. The sleeve has several holes on the lateral surface that anticipate or delay the flow of the fluid that passes through it. Holes with burrs can compromise the correct operation of the part, for this reason, it is necessary to check the presence of these unwanted elements. The industrial relevance of this problem and the need to overcome the present state of the art, which consists of a visual inspection by operators, are the reason why an automated quality control system based on machine vision, designed to detect burrs in hollow cylinders with transverse holes, was developed. The system is designed to operate on 100% production in-line.

The system developed mimics the way an operator does the inspection; the part is rotated and holes are inspected from the outside, under backlight illuminations. For the purpose, we developed a dedicated gripper, whose fingers host two cylindrical diffuse illuminators, which can be inserted inside the hollow cylinder. The part is placed orthogonal to the optical axis of the vision system and rotated around its axis so that all the holes can be imaged.
A CMOS camera equipped with a bi-telecentric lens collects images within a ROI; the holes will appear as luminous circles over a dark background. If burrs are present, their shade will appear.
Image processing is based on geometric pattern matching algorithms, which recognize circles; once a circle is identified, then deviations of its circularity are interpreted as burrs. For the purpose, deviations are analyzed versus a threshold established experimentally.
Image contrast is continuously controlled by varying the colour and intensity of the illumination, so to compensate environmental light variations typical of the factory.

The work developed has started from the analysis of the industrial problem which has led to the definition of specifications of the quality control systems to be realized. Then the thesis has addressed the conceptual and physical design of the two systems, both for the hardware and for the software.
Particular care has been put to implement adaptive behaviours, realized through specific hardware and algorithms, which aim to minimize measurement uncertainty and improve diagnostic output.
All these activities have brought to the development of laboratory prototypes, which have been characterized in laboratory conditions. They fully satisfied the expected specifications.
Then the work has continued towards the integration of the two systems to a real production line, by interfacing the systems to the tool machines; robot arms have been used to pick and place the parts. Once installed in-line, the two systems have been successfully operated for several weeks, thus providing a demonstration of their potential.

Chapter 6

List of Publications originated from this thesis

[1] Fitti M., Castellini P., Paone N., Chiariotti P. (Università Politecnica delle Marche), Zannini M., Zitti S., Gambini M. (Zannini), In-Line Burr Inspection Through Backlight Vision, 20th International Conference on IMAGE ANALYSIS AND PROCESSING, Trento, 10 September 2019

[2] Chiariotti P., Fitti M., Castellini P., Paone N. (Università Politecnica delle Marche), Zitti S., Zannini M. (Zannini), Smart quality control station for non-contact measurement of cylindrical parts based on confocal chromatic sensor, IEEE Instrumentation & Measurement Magazine Year2018 Volume 21.

[3] Chiariotti P., Fitti M., Castellini P., Paone N. (Università Politecnica delle Marche), Zitti S., Zannini M. (Zannini), High-accuracy dimensional measurement of cylindrical components by an automated test station based on confocal chromatic sensor, 2018 IEEE International Workshop on Metrology for Industry 4.0 & IoT, Brescia, 17 April 2018

[4] Chiariotti P., Fitti M., Castellini P., Paone N. (Università Politecnica delle Marche), Zitti S., Zannini M. (Zannini), High-accuracy dimensional measurement of cylindrical components by an automated test station based on confocal chromatic sensor, 2018 IEEE International Workshop on Metrology for Industry 4.0 & IoT, Brescia, 17 April 2018

References

[1] US National Science Foundation. Cyber-Physical System (CPS).

[2] Web site of EFFRA. `https://www.effra.eu/`. [accessed 28-November-2019].

[3] Web site of GO0D MAN Project. `http://go0dman-project.eu/`. [Online; accessed 24-November-2019].

[4] Web site of GRACE Project. `http://go0dman-project.eu/`. [accessed 13-March-2018].

[5] Web site of MANUFUTURE. `http://www.manufuture.org/`. [accessed 28-November-2019].

[6] Web site of Micro-Epsilon. `https://www.micro-epsilon.com/`. [accessed 25-November-2019].

[7] Web site of OPTOENGINEERING. `https://www.opto-e.com/`. [accessed 29-November-2019].

[8] Web site of Precitec. `https://www.precitec.de/en/precitec-group-start-page/`. [accessed 25-November-2019].

[9] Web site of Stil. `http://point.stil-sensors.com/`. [accessed 25-November-2019].

[10] Jan Sher Akmal. Investigation of optical distance sensors for applications in tool industry: Optical distance sensors. 2013.

[11] J.C. Aurich, D. Dornfeld, P.J. Arrazola, V. Franke, L. Leitz, and S. Min. Burrs—analysis, control and removal. *CIRP Annals*, 58(2):519 – 542, 2009.

[12] G. Berkovic, S. Zilberman, and E. Shafir. Temperature effects in chromatic confocal distance sensors. In *SENSORS, 2013 IEEE*, pages 1–3, Nov 2013.

[13] Garry Berkovic and Ehud Shafir. Optical methods for distance and displacement measurements. *Adv. Opt. Photon.*, 4(4):441–471, Dec 2012.

[14] François Blateyron. *Chromatic Confocal Microscopy*, pages 71–106. Springer Berlin Heidelberg, Berlin, Heidelberg, 2011.

[15] M. A. Browne, O. Akinyemi, and A. Boyde. Confocal surface profiling utilizing chromatic aberration. *Scanning*, 14(3):145–153, 1992.

[16] P. Castellini, C. Cristalli, M. Foehr, P. Leitao, N. Paone, I. Schjolberg, J. Tjønnås, C. Turrin, and T. Wagner. Towards the integration of process and quality control using multi-agent technology. In *IECON 2011 - 37th Annual Conference of the IEEE Industrial Electronics Society*, pages 421–426, Nov 2011.

[17] Paolo Castellini, Andrea Bruni, and Nicola Paone. Design of an optical scanner for real time on-line measurement of wood-panel profiles. In Wolfgang Osten, Christophe Gorecki, and Erik L. Novak, editors, *Optical Measurement Systems for Industrial Inspection V*, volume 6616, pages 1274 – 1285. International Society for Optics and Photonics, SPIE, 2007.

[18] Sungdo Cha, Paul C. Lin, Lijun Zhu, Pang-Chen Sun, and Yeshaiahu Fainman. Nontranslational three-dimensional profilometry by chromatic confocal microscopy with dynamically configurable micromirror scanning. *Appl. Opt.*, 39(16):2605–2613, Jun 2000.

[19] P. Chiariotti, M. Fitti, P. Castellini, S. Zitti, M. Zannini, and N. Paone. High-accuracy dimensional measurement of cylindrical components by an automated test station based on confocal chromatic sensor. In *2018 Workshop on Metrology for Industry 4.0 and IoT*, pages 58–62, April 2018.

[20] P. Chiariotti, M. Fitti, P. Castellini, S. Zitti, M. Zannini, and N. Paone. Smart quality control station for non-contact measurement of cylindrical parts based on a confocal chromatic sensor. *IEEE Instrumentation Measurement Magazine*, 21(6):22–28, December 2018.

[21] P. Chiariotti, G. M. Revel, and M. Martarelli. Exploiting continuous scanning laser doppler vibrometry and wavelet processing for damage detection. In James De Clerck, editor, *Experimental Techniques, Rotating Machinery, and Acoustics, Volume 8*, pages 189–196, Cham, 2015. Springer International Publishing.

[22] H. S. Cho and S. Chi. An inspection method for burrs in an inlet side hole using a low cost vision system. In *2015 International Conference on Information and Communication Technology Convergence (ICTC)*, pages 783–786, Oct 2015.

[23] Byung Seon Chun, Kwangsoo Kim, and Daegab Gweon. Three-dimensional surface profile measurement using a beam scanning chromatic confocal microscope. *Review of Scientific Instruments*, 80(7):073706, 2009.

[24] Joseph Cohen-Sabban, Jerome Gaillard-Groleas, and Pierre-Jean Crepin. Quasi-confocal extended field surface sensing. In Angela Duparre and Bhanwar Singh, editors, *Optical Metrology Roadmap for the Semiconductor, Optical, and Data Storage Industries II*, volume 4449, pages 178 – 183. International Society for Optics and Photonics, SPIE, 2001.

[25] C. Cristalli, M. Foehr, T. Jäger, P. Leitao, N. Paone, P. Castellini, C. Turrin, and I. Schjolberg. Integration of process and quality control using multi-agent technology. In *2013 IEEE International Symposium on Industrial Electronics*, pages 1–6, May 2013.

[26] C. Cristalli, N. Paone, and R.M. Rodríguez. Mechanical fault detection of electric motors by laser vibrometer and accelerometer measurements. *Mechanical Systems and Signal Processing*, 20(6):1350 – 1361, 2006. Special Issue: Laser Doppler Vibrometry.

[27] Sarah L. Dobson, Pang chen Sun, and Yeshayahu Fainman. Diffractive lenses for chromatic confocal imaging. *Appl. Opt.*, 36(20):4744–4748, Jul 1997.

[28] G D'Emilia, D Di Gasbarro, A Gaspari, and E Natale. Accuracy assessment for a multiparameter optical calliper in on line automotive applications. In *Journal of Physics: Conference Series*, volume 882, page 012007. IOP Publishing, 2017.

[29] Giulio D'Emilia, Giuseppe Di Rosso, Antonella Gaspari, and Alessandra Massimo. Metrological interpretation of a six-sigma process for improving the online optical measurement of automotive turbocharger dimensions. *Proceedings of the Institution of Mechanical Engineers, Part D: Journal of Automobile Engineering*, 229(2):261–269, 2015.

[30] Joint Committee for Guides in Metrology. Jcgm 100: Evaluation of measurement data - guide to the expression of uncertainty in measurement. Technical report, JCGM, 2008.

[31] J. Galas, D. Litwin, T. Kozłowski, S. Sitarek, and N. Błocki. Confocal techniques for surface profile measurements - methodology and instrumentation. *Problemy Eksploatacji*, nr 4:105–113, 2006.

[32] Johnson Garzón, Tijani Gharbi, and Jaime Meneses. Real time determination of the optical thickness and topography of tissues by chromatic confocal microscopy. *Journal of Optics A: Pure and Applied Optics*, 10(10):104028, sep 2008.

[33] Martin Gavrilov, Piotr Indyk, Rajeev Motwani, and Suresh Venkatasubramanian. Geometric pattern matching: A performance study. In *Proceedings of the Fifteenth Annual Symposium on Computational Geometry*, SCG '99, pages 79–85, New York, NY, USA, 1999. ACM.

[34] Min Gu and Colin Sheppard. Signal level of the fibre-optical confocal scanning microscope. *Journal of Modern Optics - J MOD OPTIC*, 38:1621–1630, 08 1991.

[35] Reinhold Hoenicka and Alexander Fink. Method for compensating for temperature related measurement errors in a confocal chromatic measuring distance sensor, August 21 2012. US Patent 8,248,598.

[36] ISO Central Secretary. Technical product documentation – edges of undefined shape – indication and dimensioning. Standard ISO 13715:2017, International Organization for Standardization, Geneva, CH, 2017.

[37] R. Juškaitis and T. Wilson. Imaging in reciprocal fibre-optic based confocal scanning microscopes. *Optics Communications*, 92(4):315 – 325, 1992.

[38] Matthias Kunkel, Jochen Schulze, Markus Kogel-Hollacher, and Susan Sprentall. Non-contact measurement of central lens thickness. *International Congress on Applications of Lasers & Electro-Optics*, 2005(1):1502, 2005.

[39] Paulo Leitão and Nelson Rodrigues. Multi-agent system for on-demand production integrating production and quality control. In Vladimír Mařík, Pavel Vrba, and Paulo Leitão, editors, *Holonic and Multi-Agent Systems for Manufacturing*, pages 84–93, Berlin, Heidelberg, 2011. Springer Berlin Heidelberg.

[40] Shiguang Li, Todd Thorsen, Zhiguang Xu, Zhong Ping Fang, Jianhong Zhao, and Soon Fatt Yoon. Microvalve thickness and topography measurements in microfluidic devices by white-light confocal microscopy. *Appl. Opt.*, 48(27):5088–5094, Sep 2009.

[41] Paul C. Lin, Pang-Chen Sun, Lijun Zhu, and Yeshaiahu Fainman. Single-shot depth-section imaging through chromatic slit-scan confocal microscopy. *Appl. Opt.*, 37(28):6764–6770, Oct 1998.

[42] D. Litwin, J. Galas, S. Sitarek, B. Surma, B. Piatkowski, and A. Miros. Temperature influence in confocal techniques for a silicon wafer testing. In Francesco Baldini, Jiri Homola, Robert A. Lieberman, and Miroslav Miler, editors, *Optical Sensing Technology and Applications*, volume 6585, pages 247 – 254. International Society for Optics and Photonics, SPIE, 2007.

[43] Peter Lücke, Arndt Last, and Jürgen Mohr. *Mikrooptische Sensoren nach dem chromatisch konfokalen Messprinzip*. 2006.

[44] Peter Luecke, Arndt Last, Juergen Mohr, Aiko Ruprecht, Wolfgang Osten, Hans J. Tiziani, and Peter Lehmann. Confocal micro-optical distance sensor for precision metrology. In Brian Culshaw, Anna Grazia Mignani, and Rainer Riesenberg, editors, *Optical Sensing*, volume 5459, pages 180 – 184. International Society for Optics and Photonics, SPIE, 2004.

[45] L. Mari and D. Petri. The metrological culture in the context of big data: managing data-driven decision confidence. *IEEE Instrumentation Measurement Magazine*, 20(5):4–20, October 2017.

[46] Minsky Marvin. Microscopy apparatus, December 19 1961. (filed 7. Nov. 1957).

[47] John McBride and Christian Maul. The 3d measurement and analysis of high precision surfaces using con-focal optical methods. *IEICE Transactions on Electronics*, E87-C(8):1261–1267, 2004.

[48] Antonin Miks, Jiri Novak, and Pavel Novak. Analysis of method for measuring thickness of plane-parallel plates and lenses using chromatic confocal sensor. *Appl. Opt.*, 49(17):3259–3264, Jun 2010.

[49] G. Molesini, G. Pedrini, P. Poggi, and F. Quercioli. Focus-wavelength encoded optical profilometer. *Optics Communications*, 49(4):229 – 233, 1984.

[50] M.A. Montironi, P. Castellini, L. Stroppa, and N. Paone. Adaptive autonomous positioning of a robot vision system: Application to quality control on production lines. *Robotics and Computer-Integrated Manufacturing*, 30(5):489 – 498, 2014.

[51] H Nouira, N El-Hayek, X Yuan, and N Anwer. Characterization of the main error sources of chromatic confocal probes for dimensional measurement. *Measurement Science and Technology*, 25(4):044011, mar 2014.

[52] Hichem Nouira, Nadim El Hayek, X. Yuan, Nabil Anwer, and José Salgado. Metrological characterization of optical confocal sensors measurements (20 and 350 travel ranges). *IoP Journal of Physics: Conference Series*, 483, 03 2014.

[53] Jiri Novak and Antonin Miks. Hyperchromats with linear dependence of longitudinal chromatic aberration on wavelength. *Optik*, 116(4):165 – 168, 2005.

[54] M. Fitti N. Paone M. Zannini S.Zitti. P. Castellini, P. Chiariotti. Sistema per rilevamento di bave di lavorazione in componenti meccanici, March 26 2018. Italian patent application pending No. 102018000003929.

[55] Foivos Psarommatis, Gökan May, Paul-Arthur Dreyfus, and Dimitris Kiritsis. Zero defect manufacturing: state-of-the-art review, shortcomings and future directions in research. *International Journal of Production Research*, 0(0):1–17, 2019.

[56] J Garzón R, J Meneses, G Tribillon, T Gharbi, and A Plata. Chromatic confocal microscopy by means of continuum light generated through a standard single-mode fibre. *Journal of Optics A: Pure and Applied Optics*, 6(6):544–548, apr 2004.

[57] Johnson Garzon Reyes, J. Meneses, Arturo Plata, Gilbert M. Tribillon, and Tijani Gharbi. Chromatic confocal method for determination of the refractive index and thickness. In Aristides Marcano O. and Jose Luis Paz, editors, *5th Iberoamerican Meeting on Optics and 8th Latin American Meeting on Optics, Lasers, and Their Applications*, volume 5622, pages 805 – 810. International Society for Optics and Photonics, SPIE, 2004.

[58] Giovanni B. Rossi and Francesco Crenna. A probabilistic approach to measurement-based decisions. *Measurement*, 39(2):101 – 119, 2006.

[59] A. K. Ruprecht, T. F. Wiesendanger, and H. J. Tiziani. Chromatic confocal microscopy with a finite pinhole size. *Opt. Lett.*, 29(18):2130–2132, Sep 2004.

[60] Aiko K. Ruprecht, Klaus Koerner, Tobias F. Wiesendanger, Hans J. Tiziani, and Wolfgang Osten. Chromatic confocal detection for high-speed microtopography measurements. In Brian D. Corner, Peng Li, and Roy P. Pargas, editors, *Three-Dimensional Image Capture and Applications VI*, volume 5302, pages 53 – 60. International Society for Optics and Photonics, SPIE, 2004.

[61] Aiko K. Ruprecht, Klaus Körner, Tobias F. Wiesendanger, Hans J. Tiziani, Wolfgang Osten Prof. Dr. sc. nat., Peter Lücke, and Internationales Wissenschaftliches Kolloquium (IWK). Technische Universität Ilmenau ; 50 (Ilmenau) : 2005.09.19-23. Chromatic confocal sensors for micro-topography measurements. *Maschinenbau von Makro bis Nano: 50. Internationales Wissenschaftliches Kolloquium, September, 19 - 23, 2005 ; proceedings*, 50, 2005:[05.2.03], Dec 2010. CD-ROM-Ausg.: Tagungsunterlagen / Technische Universität Ilmenau, Fakultät für Maschinenbau = Proceedings / Technische Universität Ilmenau, Faculty of Mechanical Engineering : 50. IWK, 19. - 23.09.2005 ; IMEKO 21. - 24.09.2005 ; AMAM 25. - 30.09.2005 / [Hrsg.: Peter Scharff] Ilmenau : Techn. Univ., 2005 ISBN 3-932633-99-7 Kongress: Internationales Wissenschaftliches Kolloquium. Technische Universität Ilmenau, IWK ; 50 (Ilmenau) : 2005.09.19-23. Die CD-ROM enthält zusätzlich die Vorträge der Tagungen IMEKO und AMAM. Tagungsband mit den Kurzfassungen der Konferenzbeiträge u.d.T.: Mechanical engineering from macro to nano. - Ilmenau : Verl. ISLE, 2005. - ISBN 3-932633-98-9.

[62] Aiko K. Ruprecht, Christof Pruss, Hans J. Tiziani, Wolfgang Osten, Peter Lucke, Arndt Last, Jurgen Mohr, and Peter Lehmann. Confocal micro-optical distance sensor: principle and design. In Wolfgang Osten, Christophe Gorecki, and Erik L. Novak, editors, *Optical Measurement Systems for Industrial Inspection IV*, volume 5856, pages 128 – 135. International Society for Optics and Photonics, SPIE, 2005.

[63] Aiko K. Ruprecht, Christof Pruss, Hans J. Tiziani, Wolfgang Osten, Peter Lucke, Arndt Last, Jurgen Mohr, and Peter Lehmann. Confocal micro-optical distance sensor: principle and design. In Wolfgang Osten, Christophe Gorecki, and Erik L. Novak, editors, *Optical Measurement Systems for Industrial Inspection IV*, volume 5856, pages 128 – 135. International Society for Optics and Photonics, SPIE, 2005.

[64] Kebin Shi, Peng Li, Shizhuo Yin, and Zhiwen Liu. Chromatic confocal microscopy using supercontinuum light. *Opt. Express*, 12(10):2096–2101, May 2004.

[65] L. Stroppa, P. Castellini, and N. Paone. Self-optimizing robot vision for online quality control. *Experimental Techniques*, 40(3):1051–1064, Jun 2016.

[66] Boonsong Sutapun, Armote Somboonkaew, Ratthasart Amarit, and Sataporn Chanhorm. Development and beam-shape analysis of an integrated fiber-optic confocal probe for high-precision central thickness measurement of small-radius lenses. *Sensors*, 15:8512–8526, 04 2015.

[67] Agilent Technologies. Light guide techniques using led lamps. *Application Brief I-0003*, page 22 pages, Copyright 2001.

[68] H. J. Tiziani, R. Achi, R. N. Krämer, and L. Wiegers. Theoretical analysis of confocal microscopy with microlenses. *Appl. Opt.*, 35(1):120–125, Jan 1996.

[69] H. J. Tiziani, R. Achi, and R. N. Krämer. Chromatic confocal microscopy with microlenses. *Journal of Modern Optics*, 43(1):155–163, 1996.

[70] H. J. Tiziani and H.-M. Uhde. Three-dimensional image sensing by chromatic confocal microscopy. *Appl. Opt.*, 33(10):1838–1843, Apr 1994.

[71] Hans J. Tiziani and Hans-Martin Uhde. Three-dimensional analysis by a microlens-array confocal arrangement. *Appl. Opt.*, 33(4):567–572, Feb 1994.

[72] Hans J. Tiziani, M. Wegner, and Daniela Steudle. Confocal principle for macro- and microscopic surface and defect analysis. *Optical Engineering*, 39(1):32 – 39, 2000.

[73] D.-M. Tsai. A machine vision approach for detecting and inspecting circular parts. *The International Journal of Advanced Manufacturing Technology*, 15(3):217–221, Mar 1999.

[74] A. Weckenmann, T. Estler, G. Peggs, and D. McMurtry. Probing systems in dimensional metrology. *CIRP Annals*, 53(2):657 – 684, 2004.

[75] J. H. Wray and John T. Neu. Refractive index of several glasses as a function of wavelength and temperature∗. *J. Opt. Soc. Am.*, 59(6):774–776, Jun 1969.

[76] Yan Zhao, Yiwen Wang, Xiuling Ye, Zhong Wang, Luhua Fu, Changjie Liu, and Zhiwei Wang. Multi-sensor registration in high-precision cmm based on a composite standard. *Sensors*, 18(4), 2018.